PyramidA

Monte Carlo Modeling of Pyramid Array Radiation Characteristics

Manual

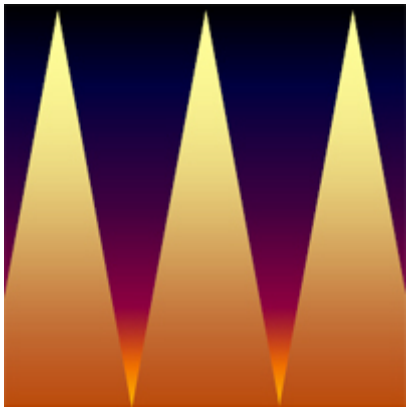

www.virial.com

CONTENT

1. INTRODUCTION

PyramidA is the program for calculating effective emissivities and radiance (a.k.a. brightness) temperatures of blackbody radiation sources operating in optical spectral range and shaped as a regular array of square-based pyramids (see Fig. 1). Pyramid array blackbodies (PABBs) are used instead of cavity-type of blackbody radiators when it is necessary to provide large radiating area with the moderate effective emissivity (about 0.95…0.99) and when the compactness is the additional requirement, as it takes place in the case of onboard calibration of satellite spectroradiometric equipment [1-4]. Some blackbody manufacturers (see, e.g., [5, 6]) offer PABBs for radiometric and thermometric calibrations from visible to far IR spectral range.

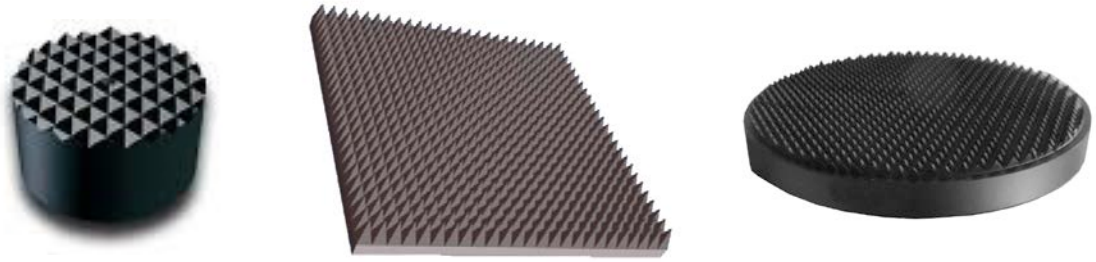

Fig. 1. Pyramid array blackbody radiators.

In the last decade, the pyramid arrays with a thin layer of epoxy-based absorber on a metal substrate became widespread as blackbody calibration sources in metrology of radiometric power and related quantities in the millimeter-wave and terahertz frequency ranges [7-11].

Although PABBs of all spectral ranges use the same effect of multiple reflections among pyramid array surfaces, the methods applicable for calculating their radiation characteristics are quite different. The characteristic size of PABB (for instance, pyramid base side) of about several millimeters is significantly greater than the wavelength within visible and infrared spectral ranges; therefore, geometrical optics approximation can be applied. For microwave spectral range, the characteristic size becomes comparable with the wavelength, so conjoint electromagnetic and thermal analyses should be performed for rigorous determination of radiation characteristics for such PABBs. Polarization effects must be also taken into account.

PyramidA uses geometrical optics and could not be applied to calculation of radiation characteristics of PABB operating outside the optical range of electromagnetic radiation (for microwave/terahertz and radio-frequency blackbody calibration targets and loads).

Regular array of square-based pyramids is sometimes used as a bottom of cylindrical blackbody cavities [12-17] to increase cavity effective emissivity as well as to make cavity bottom more diffuse what is especially important if the material of a cavity bottom has significant specular component of reflection. In such a case, PyramidA can be employed for a rough estimate of effective emissivities of the cavity bottom then these values can be used as an input for calculation of radiation characteristics of a cylindrical cavity.

Methods for calculation of radiation characteristics of PABB were not developed until now except Refs. [18-20] where the directional effective emissivity was evaluated for a purely specular pyramid array approximating a randomly rough surface.

PyramidA is the world's first software tool for exact calculation of the effective emissivities and radiance temperatures for PABB with specular-diffuse surfaces. PyramidA is intended for researchers working in optical radiometry, radiation thermometry, and adjacent areas such a remote sensing.

2. PyramidA MAIN FEATURES

PyramidA performs calculations of the spectral effective emissivities and radiance temperatures of PABB having the following properties:

- PABB is formed from a square array having n columns and n rows ($n \le 1001$) of identical pyramids or truncated pyramids (frusta) placed on the flat base, with the optional gaps of constant width between pyramids (see. Fig. 1).
- Each (truncated) pyramid has the square base and the apex above the center of the square base (see Fig. 2).
- PABB boundary can be a square or a circle; PABB center can coincide with the apex of a pyramid or with the center of a four neighbor pyramids cluster (see Figs. 3-6).
- All radiating surface of a PABB has the same optical characteristics described by the Uniform Specular-Diffuse Model (see Section 3.3).
- Spectral reflectance of the PABB surface can be defined for up to 1001 wavelengths.
- Linear temperature change can be defined along pyramid height.
- PABB base is isothermal.
- 4 types of geometrical conditions of the radiation collecting (viewing conditions) can be modeled
- The background radiation can be modeled as the perfect blackbody radiation at temperature T_{bg} uniformly falling onto PABB from the surrounding hemisphere.
- Calculation results can be presented in form of tables and graphs. Graphs are fully editable and can be copied to clipboard and saved as bitmaps (**.bmp*) or Windows metafiles (**.wmf*, **.emf*).
- Numerical results can be saved in text files, XLS-files (MS Excel spreadsheets), as XML and HTML tables.

The requirements for hardware and software are the following:

- CPU frequency 1 GHz or higher
- Screen Resolution 1152×864 or greater
- Hard disk space 10 MB minimum
- RAM 1 GB
- Operating System MS Windows XP (with SP2), Vista, 7, 8 (in compatibility mode)

3. Theoretical Basis

3.1. Definitions of Principal Quantities

A source of optical radiation whose radiation characteristics can be calculated on the basis of fundamental physical laws makes possible independent calibration of radiometers, spectroradiometers, radiation thermometers, and other measurement equipment. From theoretical point of view, a perfect blackbody is the most suitable object for this purpose because its radiation characteristics are entirely determined by its thermodynamic temperature. However, a perfect blackbody is a physical abstraction that does not exist in real world. The perfect blackbody conditions are realized inside an isothermal cavity with opaque walls. The radiation escaping cavity through a tiny opening very closely imitates blackbody radiation. However, not only cavities are suitable for mimicking a perfect blackbody but also some other objects which output radiation undergoes multiple reflections (such as a flat surface covered with a concave mirror having a small opening, a tight wire bundle, a stack of blades, array of pyramids or conical spikes). In order to employ a blackbody as a standard reference source, it is necessary to know how large differences are between radiation characteristics of a perfect blackbody and those of a blackbody radiation source for a given geometry, material, temperature, and wavelength.

There are two different objects referred in literature as “blackbody”:

1. A theoretical object that completely absorbs all radiant energy incidents upon it. A blackbody emits maximum amount of radiant energy at given wavelength and given temperature in comparison with all other radiating bodies.
2. An artificial source of radiation designed to simulate characteristics of a perfect blackbody and used as a reference radiation source of known radiant exitance and spectral distribution of radiant power.

To distinguish them, we will use the term “***perfect blackbody***” for theoretical object, saving the term “***blackbody***” for artificial source.

Quantitative measure of difference in the radiation characteristics between an artificial blackbody and a perfect one is the effective emissivity. The qualifier ***effective*** indicates the effect produced by multiple reflections. Unlike in the case of a flat sample, outgoing radiation of an element of a blackbody surface consists not only of its own thermal radiation, but also of radiation falling from other surface elements and reflected by the element under consideration. Generally speaking, effective emissivity is the ratio of a radiometric quantity (usually, radiance or spectral radiance) that characterizes a blackbody at a certain temperature to the same quantity

of a perfect blackbody with the same temperature. Real-world blackbodies are always nonisothermal. Temperature nonuniformity can distort significantly their radiation characteristics. Effective emissivity of a nonisothermal blackbody is a function of a reference temperature assigned to a perfect blackbody in the effective emissivity definition. It might be less or greater than unity, depending on the reference temperature.

The most important quantities characterizing blackbody radiation sources are defined for the nonrefracting, nonabsorbing, nonscattering, and nonemitting environment (i.e., vacuum at 0 K). It is also assumed that the optical properties of blackbody material do not depend on temperature.

The primary characteristic of an artificial blackbody (hereinafter – blackbody, for short) is the spectral local directional effective emissivity ε_e that is defined by the following equation:

$$\varepsilon_e\left(\lambda,\boldsymbol{\xi},\boldsymbol{\omega},T_{ref}\right)=\frac{L_\lambda\left(\lambda,\boldsymbol{\xi},\boldsymbol{\omega}\right)}{L_{\lambda,bb}\left(\lambda,T_{ref}\right)}, \tag{1}$$

where L_λ is spectral radiance (in $W\cdot m^{-3}\cdot sr^{-1}$) emitted from a point on blackbody surface at a particular wavelength λ, with coordinates specified by the vector $\boldsymbol{\xi}$, and the direction in which the radiation is emitted is given by the vector $\boldsymbol{\omega}$; $L_{\lambda,bb}$ is spectral radiance of a perfect blackbody at a reference temperature T_{ref} and the same wavelength λ.

Denominator in Eq. (1) is expressed by Planck's law:

$$L_{\lambda,bb}\left(\lambda,T_{ref}\right)=\frac{c_1}{\pi\cdot\lambda^5\left[\exp\left(\frac{c_2}{\lambda\cdot T_{ref}}\right)-1\right]}, \tag{2}$$

where c_1 and c_2 are the 1st and 2nd radiation constants, respectively.

Integration over the entire spectrum together with the relative spectral responsivity $r(\lambda)$ of a detector, gives the bandlimited local directional effective emissivity:

$$\bar{\varepsilon}_e\left(\boldsymbol{\xi},\boldsymbol{\omega},T_{ref}\right)=\frac{\int_0^\infty r(\lambda)L_\lambda(\lambda,\boldsymbol{\xi},\boldsymbol{\omega})d\lambda}{\int_0^\infty r(\lambda)L_{\lambda,bb}\left(\lambda,\boldsymbol{\xi},\boldsymbol{\omega},T_{ref}\right)d\lambda}. \tag{3}$$

Integration over a hemispherical solid angle transforms the term for the spectral radiance L_λ to the spectral radiant exitance M_λ. The spectral and bandlimited hemispherical effective emissivities are defined by the following equations:

$$\varepsilon_{e,h}\left(\lambda,\boldsymbol{\xi},T_{ref}\right)=\frac{M_\lambda(\lambda,\boldsymbol{\xi})}{M_{\lambda,bb}\left(\lambda,T_{ref}\right)}=\frac{M_\lambda(\lambda,\boldsymbol{\xi})}{\pi L_{\lambda,bb}\left(\lambda,T_{ref}\right)}, \tag{4}$$

$$\bar{\varepsilon}_{e,h}\left(\boldsymbol{\xi},T_{ref}\right)=\frac{\int_0^\infty r(\lambda)M_\lambda(\lambda,\boldsymbol{\xi})d\lambda}{\int_0^\infty r(\lambda)M_{\lambda,bb}\left(\lambda,T_{ref}\right)d\lambda}=\frac{\int_0^\infty r(\lambda)M_\lambda(\lambda,\boldsymbol{\xi})d\lambda}{\pi\int_0^\infty r(\lambda)L_{\lambda,bb}\left(\lambda,T_{ref}\right)d\lambda}, \tag{5}$$

Often, knowing *the spectral integrated effective emissivity* $\varepsilon_{e,c}$ is necessary. Its value is equal to the ratio of spectral radiant flux Φ_λ falling onto the detector from a blackbody to spectral radiant flux $\Phi_{\lambda,bb}$ from a perfectly black surface with the temperature T_{ref} replacing the blackbody:

$$\varepsilon_{e,c}\left(\lambda,T_{ref}\right)=\frac{\Phi_\lambda(\lambda)}{\Phi_{\lambda,bb}\left(\lambda,T_{ref}\right)}. \tag{6}$$

Integration with $r(\lambda)$ over the entire spectrum results in bandlimited integrated effective emissivity:

$$\bar{\varepsilon}_{e,c}\left(T_{ref}\right)=\frac{\int_0^\infty r(\lambda)\Phi_\lambda(\lambda)d\lambda}{\int_0^\infty r(\lambda)\Phi_{\lambda,bb}\left(\lambda,T_{ref}\right)d\lambda}. \tag{7}$$

Depending on particular viewing conditions used for various types of radiation thermometers, pyrometers, radiometers etc., one can define the appropriate types of effective emissivities by

averaging local directional effective emissivity over a visible part of blackbody's surface and a suitable solid angle.

Radiance (or *brightness*) *temperature* T_S is defined as a temperature of a perfect blackbody, for which the spectral radiance at the specified wavelength λ has the same value as that for the thermal radiator under consideration. For a blackbody having spectral effective emissivity ε_e, the radiance temperature is equal to

$$T_S(\lambda,\boldsymbol{\xi},\boldsymbol{\omega}) = c_2\left\{\lambda\ln\left[1+\frac{\exp\left(\frac{c_2}{\lambda T_{ref}}\right)-1}{\varepsilon_e(\lambda,\boldsymbol{\xi},\boldsymbol{\omega},T_{ref})}\right]\right\}^{-1}. \tag{8}$$

The practical radiation thermometers do not measure the monochromatic spectral radiance. If $r(\lambda)$ is the relative spectral responsivity of the radiation thermometer (that is defined by the spectral transmittance of its optical components, spectral sensitivity of the radiation detector and other factors), certain "average" values will be registered. The bandlimited radiance temperature $\overline{T_S}$ can be found from the equation

$$\int_0^\infty r(\lambda)\varepsilon_e(\lambda,T_{ref})\,L_{\lambda,bb}(\lambda,T_{ref})\,d\lambda = \int_0^\infty r(\lambda)L_{\lambda,bb}(\lambda,\overline{T_S})\,d\lambda, \tag{9}$$

which has be solved numerically.

It should be noted that terms and definitions of bandlimited values are absent in standards and regulations [22, 23] as well as in other normative documents. This fact does not prevent researchers to use them (see, e.g., [24, 25]).

As mentioned above, radiation characteristics of a blackbody with inhomogeneous temperature can differ significantly from those of the isothermal blackbody. Effective emissivity of a nonisothermal blackbody radiator can be greater or less than that of isothermal one, depending on the reference temperature choice. In some cases, effective emissivity of nonisothermal blackbody can exceed unity. However, this means only that the thermal radiation of a blackbody radiation source is more intensive than that of a perfect blackbody at the reference temperature under other equal conditions. If T_{ref} and T'_{ref} are two reference temperatures, then

$$\varepsilon_e\left(\lambda,T_{ref}\right)=\varepsilon_e\left(\lambda,T'_{ref}\right)\frac{L_{\lambda,bb}\left(\lambda,T'_{ref}\right)}{L_{\lambda,bb}\left(\lambda,T_{ref}\right)}=\varepsilon_e\left(\lambda,T'_{ref}\right)\frac{\exp\left(\frac{c_2}{\lambda T'_{ref}}\right)-1}{\exp\left(\frac{c_2}{\lambda T_{ref}}\right)-1}. \tag{10}$$

All definitions above have been developed for a non-radiating background environment. However, actual environments have temperatures greater than the 0 K. Thermal radiation from surrounding irradiates a blackbody and can reach detector after multiple reflections. The simplest case of isotropic blackbody radiation corresponding to the background temperature T_{bg} is usually considered. The effect of background radiation on the spectral local directional effective emissivity of a nonisothermal blackbody is taken into account by the second term in the following equation:

$$\varepsilon_e\left(\lambda,\boldsymbol{\xi},\boldsymbol{\omega},T_{ref},T_{bg}\right)=\varepsilon_e\left(\lambda,\boldsymbol{\xi},\boldsymbol{\omega},T_{ref}\right)+\left[1-\varepsilon_e\left(\lambda,\boldsymbol{\xi},\boldsymbol{\omega}\right)\right]\frac{\exp\left(\frac{c_2}{\lambda T_{ref}}\right)-1}{\exp\left(\frac{c_2}{\lambda T_{bg}}\right)-1}, \tag{11}$$

were $\varepsilon_e\left(\lambda,\boldsymbol{\xi},\boldsymbol{\omega},T_{ref},T_{bg}\right)$ is the nonisothermal blackbody spectral effective emissivity with the account of background radiation; $\varepsilon_e\left(\lambda,\boldsymbol{\xi},\boldsymbol{\omega},T_{ref}\right)$ does not include this correction; $\varepsilon_e\left(\lambda,\boldsymbol{\xi},\boldsymbol{\omega}\right)$ is spectral effective emissivity of the isothermal blackbody.

By analogy, the bandlimited effective emissivity of a nonisothermal blackbody in the presence of background radiation can be defined by the equation:

$$\overline{\varepsilon}_e\left(\boldsymbol{\xi},\boldsymbol{\omega},T_{ref},T_{bg}\right)=\frac{\int_0^\infty r(\lambda)\varepsilon_e\left(\lambda,\boldsymbol{\xi},\boldsymbol{\omega},T_{ref},T_{bg}\right)L_{\lambda,bb}\left(\lambda,T_{ref}\right)d\lambda}{\int_0^\infty r(\lambda)L_{\lambda,bb}\left(\lambda,T_{ref}\right)d\lambda}. \tag{12}$$

The bandlimited radiance temperature $\overline{T}_{S,bg}$ of a nonisothermal blackbody in the presence of background radiation can be defined by analogy with Eq. (9):

$$\int_0^\infty r(\lambda)\overline{\varepsilon}_e\left(\lambda,T_{ref},T_{bg}\right)L_{\lambda,bb}d\lambda=\int r(\lambda)L_{\lambda,bb}\left(\lambda,\overline{T}_{S,bg}\right)d\lambda, \tag{13}$$

which also should be solved numerically for $\overline{T}_{S,bg}$.

3.2. Radiator's Geometry

PyramidA deals with blackbody radiators formed by an array of identical square-based pyramids or truncated pyramids densely or with equal gaps regularly arranged on the flat base surface (see Fig. 1). Fig. 2 shows an individual pyramid (frustum); its dimensions are presented in Fig. 3.

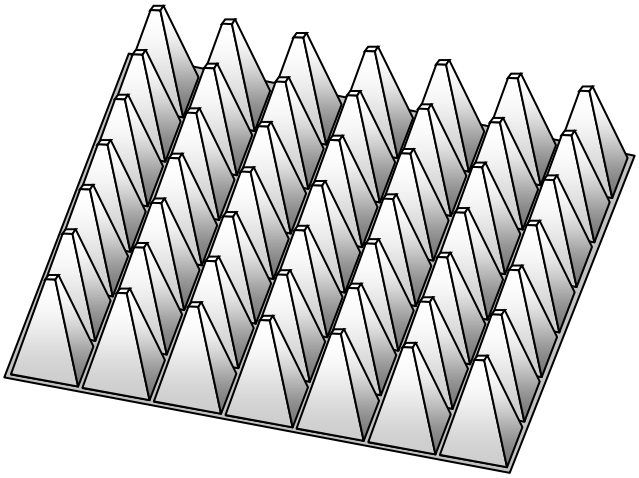

Fig. 1. An example of a 7×7 square-based pyramid array.

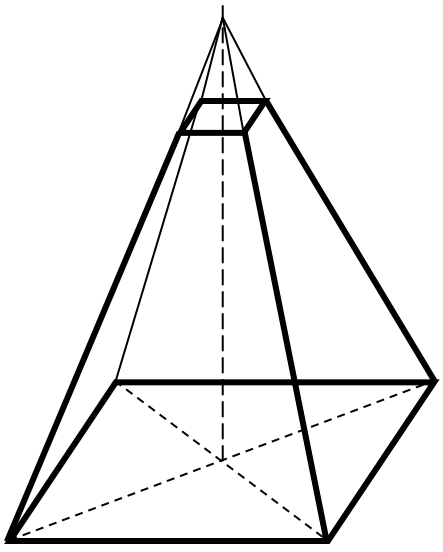

Fig. 2. An individual pyramid (frustum).

PyramidA allows modeling PABB with square (see Figs. 3 and 4) or circular (Figs. 5 and 6) boundaries. PABB center may coincide with the pyramid vertex (see Figs. 3 and 5) or with the center of inter-pyramid gaps crossroad (Figs. 4 and 6).

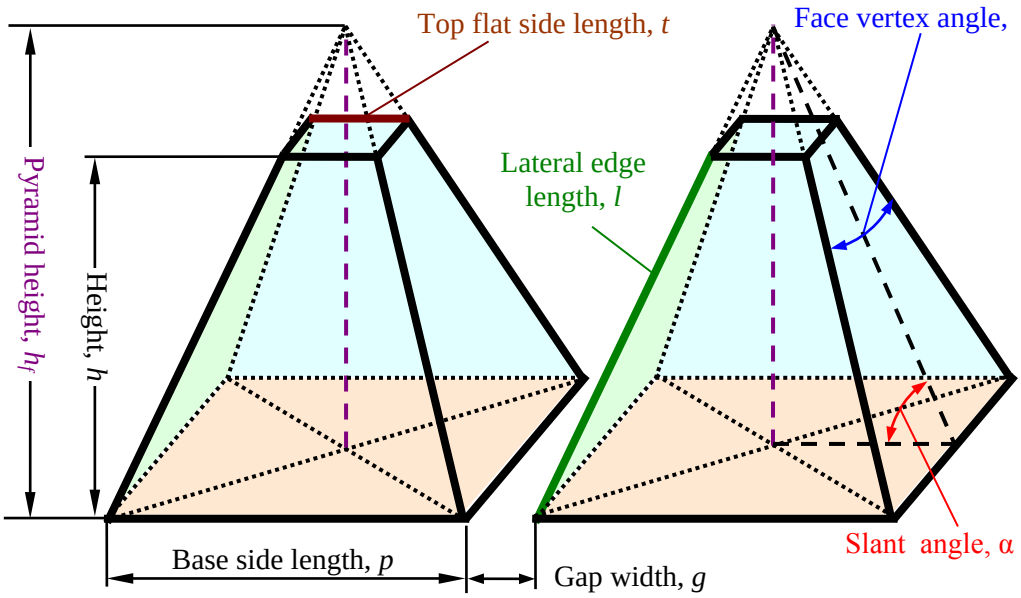

Fig. 3. Pyramid dimensions.

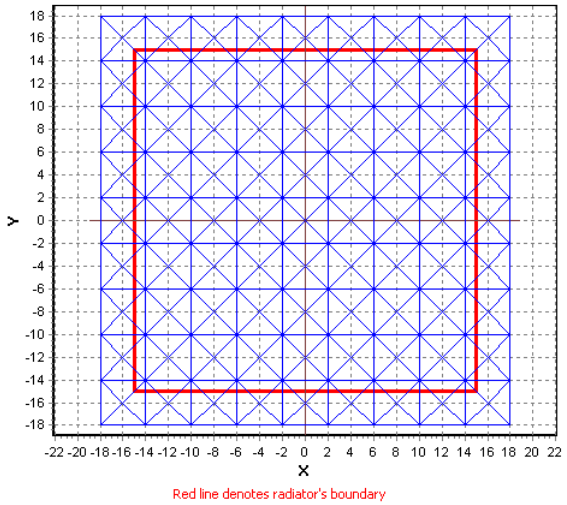

Fig. 3. Square PABB; radiator's center coincides with the pyramid vertex.

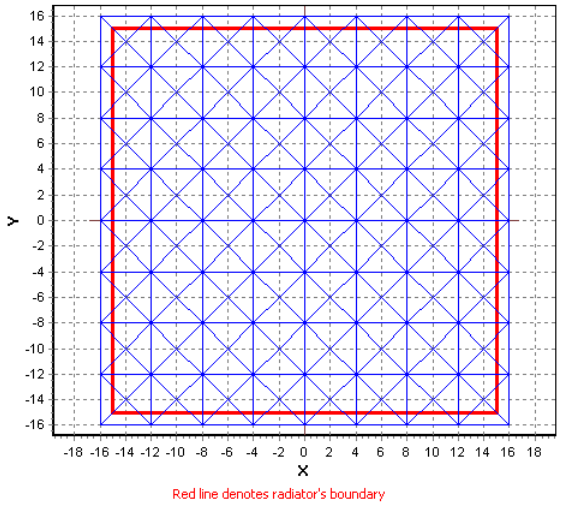

Fig. 4. Square PABB; radiator's center coincides with the inter-pyramid valley crossing.

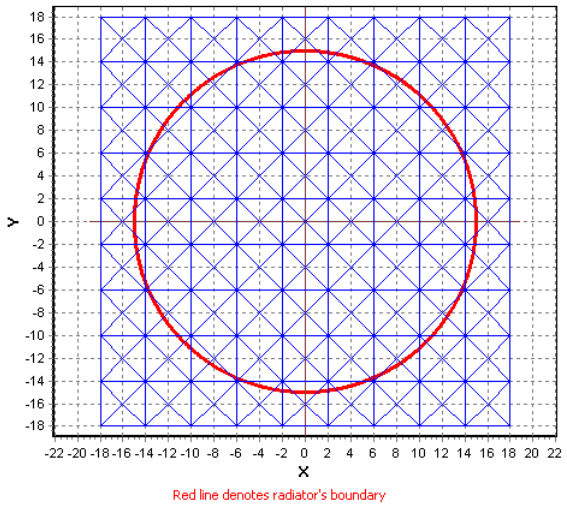

Fig. 5. Circular PABB; radiator's center coincides with the pyramid vertex.

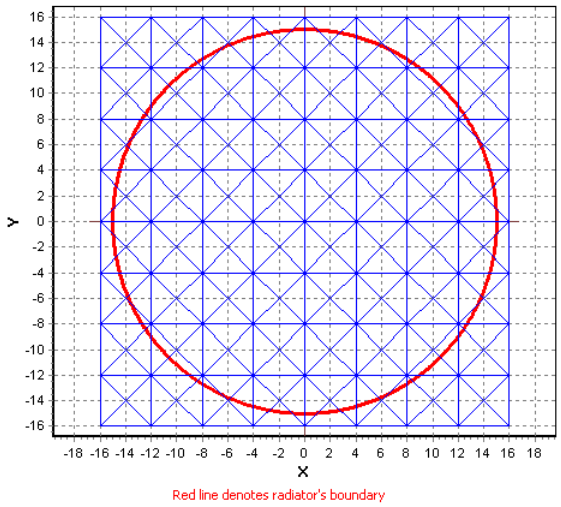

Fig. 6. Circular PABB; radiator's center coincides with the inter-pyramid valley crossing.

Geometry of PABB is completely described by the following input dimensions:

- Radiator diameter or square side *D*
- Pyramid base side length *p*
- Pyramid top flat side *t*
- Gap width *g*
- Pyramid lateral face slant angle α

Other geometric values are considered as auxiliary parameters and can be expressed in terms of input dimensions:

- Array period $c = p + g$
- Pyramid height $h_f = \frac{1}{2} p \cdot \tan\alpha$
- Frustum height $h = \frac{1}{2}(p - t) \cdot \tan\alpha$
- Lateral face vertex angle $\beta = \tan^{-1}\left(p \Big/ \sqrt{p^2 + h_f^2}\right)$
- Array size (number or columns and rows in the array) N :

$$N = \begin{cases} \lceil D/c - \frac{1}{2} \rceil + 1, & \text{if radiator's center coincides with the pyramid vertex} \\ \lceil D/c \rceil, & \text{if radiator's center lies between pyramids} \end{cases}$$

Here $\lceil x \rceil$ is the ceiling function that is the is the smallest integer not less than x.

3.3. Uniform Specular-Diffuse Model of Reflection

The quality of the Monte Carlo modeling depends to a great extent on adequacy of stochastic model adopted for optical properties of materials that form a blackbody radiation source. The very simple and useful (but often insufficient) model is the diffuse model of reflection, which considers all materials as Lambertian emitters and reflectors. The most powerful models should take into account bi-directional reflectance distribution function (BRDF) that describes angular distributions of reflected radiation for every direction of incident radiation. However, such an approach is complicated and requires significant computational resources; besides, frequently, the experimental data required for such a model is incomplete or absent. The specular-diffuse model of reflection representing BRDF as a sum of the Lambertian (diffuse) and specular components is a reasonable trade-off, suitable for the Monte Carlo modeling of radiation characteristics of blackbodies. PyramidA employs the Uniform Specular-Diffuse (USD) model of reflection.

The specular-diffuse model of reflection has been introduced in Ref. [26]. The term "uniform specular-diffuse" was coined by A. Ono [27]. Uniform Specular-Diffuse (USD) model of reflection represents radiation reflected from a surface as a sum of two components – diffuse and specular – that do not depend on incidence angle, i.e., spectral directional-hemispherical reflectance (DHR) $\rho(\lambda)$ can be a function only of a wavelength. For all wavelengths, proportion of diffuse $\rho_d(\lambda)$ and specular $\rho_s(\lambda)$ components is the constant value:

$$\rho(\lambda) = \rho_d(\lambda) + \rho_s(\lambda), \tag{14}$$

$$\rho_d(\lambda) = \rho(\lambda) D, \tag{15}$$

$$\rho_s(\lambda) = \rho(\lambda)(1 - D), \tag{16}$$

$$D = Const, \tag{17}$$

where D is the *diffusity* (not to be confused with the *diffusivity*!)

Diffusity D does not depend on wavelength nor incidence angle. According to Kirchhoff's law, for opaque materials, spectral emissivity can be expressed as

$$\varepsilon(\lambda) = 1 - \rho(\lambda). \tag{18}$$

3.4. Radiator's Temperatures

PyramidA allows accounting for temperature change along pyramid height. As a rule, pyramid vertices are colder than their base. This temperature drop inevitably appears for most of the PABB even in vacuum environment due to different radiative heat losses at the base of pyramid and at its vertex (or flat top, for truncated pyramid). However, PyramidA imposes no restrictions on the ratio between the vertex (or flat top) temperature T_{top} and the base temperature T_{base}. It is only supposed that temperature changes linearly from T_{base} to T_{top}; temperature of entire PABB base is supposed to be uniform and equal to T_{base}.

It is recommended to choose $\mathrm{Max}(T_{base}, T_{top})$ value for the reference temperature T_{ref}; in such a case, all values of spectral effective emissivities will be less than unity (what is more familiar, no more) for any reasonable background temperatures T_{bg}.

3.5. Viewing Conditions

Effective emissivities as well as the radiance temperatures depend on *viewing conditions,* i.e., geometrical conditions of collecting the radiation by a measurement device. The appropriate effective emissivities can be obtained by averaging primary (local directional) effective emissivities over certain spatial and angular domains. Four types of viewing conditions are implemented in the PyramidA:

- Directional A,
- Directional B,
- Conical,
- Integrated.

Directional A and B viewing conditions correspond to the collimated beams of radiation emitted by the PABB. Such viewing conditions are approximately implemented if measurements are conducted using very long focal-length optics.

Conical viewing conditions correspond to the PABB radiation collecting within convergent conical beam. Such a case is realized if radiation detector uses an optical system (e. g., the objective lens) whose focal point is placed in front of a blackbody.

Integrated viewing conditions are realized when there are no diaphragms and optical system between PABB and radiation detector.

3.5.1. Line of Sight

In distinct of the most of the blackbody cavity sources, PABB is anisotropic; it has no rotational symmetry but only two mutually perpendicular planes of symmetry. This means that the effective emissivity of PABB will depend on not only the angle between the normal to the base plane and direction of observation but also on azimuthal angle. The last dependence is periodical, with the period of 90°. We'll introduce the Cartesian coordinate system as it is shown in Fig.7: the axis *Z* is normal to the PABB base plane; axes *X* and *Y* are parallel to the array rows and columns. The planes *XZ* and YZ are two symmetry planes of PABB.

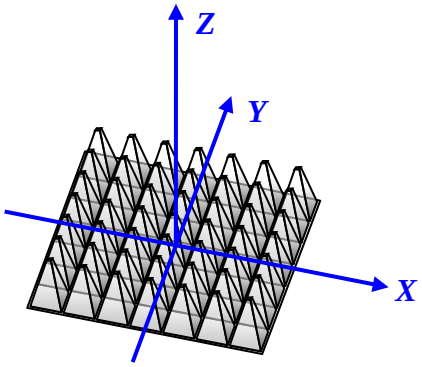

Fig. 7. Cartesian coordinate systems associated with the PABB.

PyramidA models the axially-symmetrical viewing beams for all viewing conditions types. Thus, it is necessary to define the direction of the beam axis, so-called line of sight (LoS). It is supposed that LoS starts from the coordinate system origin. By introducing the spherical coordinate system associated with the Cartesian coordinate system that was introduced previously, one can define the LoS direction by the polar angle *b* and azimuthal angle *a* as it is shown in Fig. 8 ($0° \le a < 180°$, $0° \le b < 90°$).

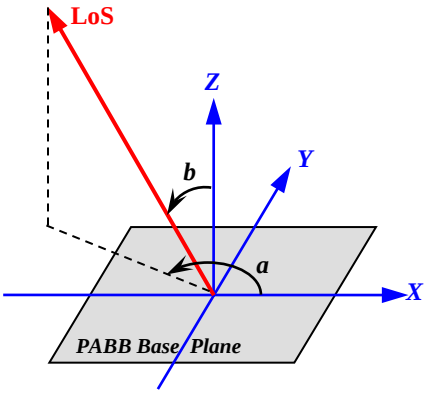

Fig. 8. Cartesian and spherical coordinate systems associated with the PABB. Line of Sight (LoS) is defined by the polar (b) and azimuthal (a) angles in spherical coordinates.

3.5.2. Directional A Viewing Conditions

The Directional A type of viewing conditions (see Fig. 9) implies that the thermal radiation from only central circular area of the PABB emitted in directions parallel to the LoS reaches the detector. This type of viewing conditions is not quite realistic in general because the viewing beam perpendicular section has elliptical shape. However, the Directional A type of viewing conditions approximates the case of very long-focus optical system and small angles *b* when only diameter of the "*footprint*" *DA* is given. This is the common case for PABBs that are used for calibration of onboard Fourier transform spectroradiometers.

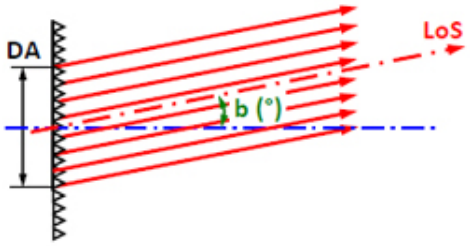

Fig. 9. Directional A viewing conditions type.

If *b* = 0° the cross-section of the viewing beam becomes circular and the Directional A becomes identical with the Directional B type of viewing condition.

3.5.3. Directional B Viewing Conditions

The Directional B type of viewing conditions (Fig. 9) considers the viewing beam as collimated, with the circular cross-section of diameter *DB*. Viewing beam diameter can be defined by the external diaphragm whose plane is perpendicular to the LoS.

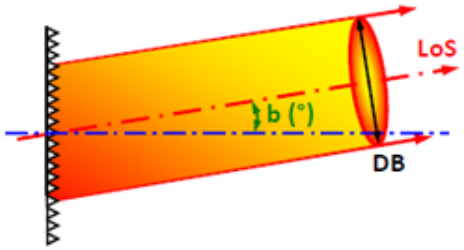

Fig. 10. Directional B viewing conditions type.

The *footprint* (the section of the viewing beam by the PABB base) has elliptical shape if *b* > 0°. This case is also implemented approximately when the focal length of the optical system is much greater than *DB*.

3.5.4. Conical Viewing Conditions

Fig. 11 presents the Conical type of viewing conditions. This is a case of observing the PABB by the radiometer, spectroradiometer, or radiation thermometer within convergent radiation beam. Focal point (conical beam vertex) lies in front of the PABB. The f*ootprint* is elliptical if *b* > 0°.

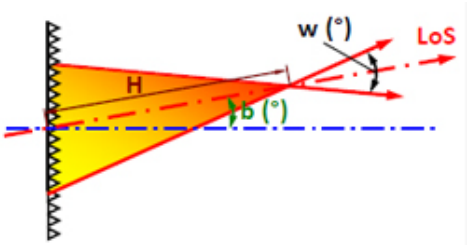

Fig. 11. Conical viewing condition type.

This type of viewing conditions is suitable for modeling of collecting PABB radiation using an optical system such an objective length or a Cassegrain reflector. In fact, optical system is modeled as a pinhole camera. This approximation is more than sufficient for most practical applications.

3.5.5. Integrated Viewing Conditions

Integrated type of viewing conditions (Fig. 12) correspond to the case of registration of the PABB radiation by circular detector of diameter *DD* placed in the plane perpendicular to LoS at the finite distance *H* to the PABB base center. In distinct of previous types of viewing conditions, each point of the detector can “see” each point of the PABB (except points masked by pyramid upper parts).

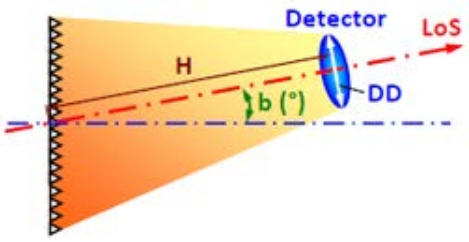

Fig. 12. Integrated viewing conditions type.

3.6. Computational Method

Direct measurements of effective emissivity of blackbodies are always difficult and often impossible. Sometimes, computational methods are the only way to determine the effective emissivity. Moreover, calculation of the effective emissivities should be done at the design stage. Many computational methods have been developed to this end (see Refs. [28, 29]) since 1950ths. These methods are based on the various physical and mathematical assumptions, have different areas of applicability and provide different levels of precision. Presently, the Monte Carlo method is the most general, developed, and flexible method for calculation of the effective emissivity. It is based on the ray tracing algorithms which simulate radiation heat transfer within framework of the ray (geometrical) optics approximation. Such phenomena as polarization and diffraction are ignored.

Detailed description of the theoretical background and examples of application of the Monte Carlo method to the effective emissivities of blackbody radiators can be found in Refs. [30, 31]. Effective emissivity calculations are based on the optical reciprocity theorem, the technique of backward ray tracing, and the method of statistical weights. A ray with statistical weight equal to unity is directed from the point of observation into the blackbody. The ray history is being traced until it leaves the blackbody after reflection from its walls, or until its statistical weight becomes less then the given value (radiant flux threshold). The last point of reflection is considered to be a birth point of a ray propagating in the opposite direction. By choosing the reference temperature T_{ref} and analyzing the history of a large number n of rays, one can evaluate the spectral effective emissivities of a blackbody for given wavelength, viewing conditions and reference temperature. If optical properties are the same throughout the blackbody radiating surface, the effective emissivity can be expressed as

$$\varepsilon_e\left(\lambda,T_{ref},T_{bg}\right)=\frac{1}{n}\left(e^{\frac{c_2}{\lambda T_{ref}}}-1\right)\sum_{i=1}^{n}\left\{\rho^{m_i}\left(\lambda\right)\left(e^{\frac{c_2}{\lambda T_{bg}}}-1\right)^{-1}+\varepsilon\left(\lambda\right)\rho^{m_i-1}\left(\lambda\right)\sum_{j=1}^{m_i}\left(e^{\frac{c_2}{\lambda T_{i,j}}}-1\right)^{-1}\right\}, \qquad (19)$$

where m_i is the number of ray reflections in the i^{th} trajectory; λ is the wavelength; c_2 is the second radiation constant in Planck's law; $\varepsilon(\lambda)$ and $\rho(\lambda)$, are the spectral emissivity and the spectral reflectance of the blackbody radiating surface, respectively; $T_{i,j}$ is the temperature in the j^{th} point of reflection of the i^{th} trajectory.

PyramidA employs the time-saving algorithm allowing calculation of the spectral effective emissivity values for isothermal and non-isothermal PABB for all wavelengths at one run. This leads to strong correlation of random errors for computed spectral emissivities. In practice, this

does not lead to any problems; however, it must be noted that the smoothness of spectral emissivity curves by itself cannot guarantee high accuracy of the calculation results.

After calculation of spectral emissivities, the radiance temperatures for each wavelength can be computed using the following expression:

$$T_S\left(\lambda, T_{bg}\right) = c_2 \left\{ \lambda \ln\left[1 + \left(e^{\frac{c_2}{\lambda T_{ref}}} - 1 \right) \varepsilon_e^{-1}\left(\lambda, T_{ref}, T_{bg}\right) \right] \right\}^{-1} . \quad (20)$$

4. Measurement Units and Fundamental Physical Constants

PyramidA uses the International System of Units (SI). Below, the table with the units of physical quantities that PyramidA uses is shown.

Quantity	Unit	Comments
Linear dimensions	Arbitrary	All the PABB and viewing conditions linear dimensions must be expressed in the same units
Wavelength	Micrometer	1 μm = 10^{-6} m
Angular dimensions	Degree, °	$1^\circ = \pi/180 \approx$ 0.0174532925 rad
Temperature	Kelvin, K	Conversion formulae: [K] = [°C] + 273.15; [K] = ([°F] + 459.67) × $5/9$

The following value of the 2nd radiation constant in Planck's law is used (see Ref. [21]):

$$c_2 = 1.4387752\times10^{-2}\ \text{m·K}.$$

5. WORKING WITH PyramidA

5.1. Installation of PyramidA

PyramidA does not require special efforts for installation. Simply download the Evaluation version of the program from www.virial.com, unzip *PyramidA.zip* to any place of the hard drive without changing the structure of *PyramidA* folder, and run *PyramidA.exe*. The main window will appear:

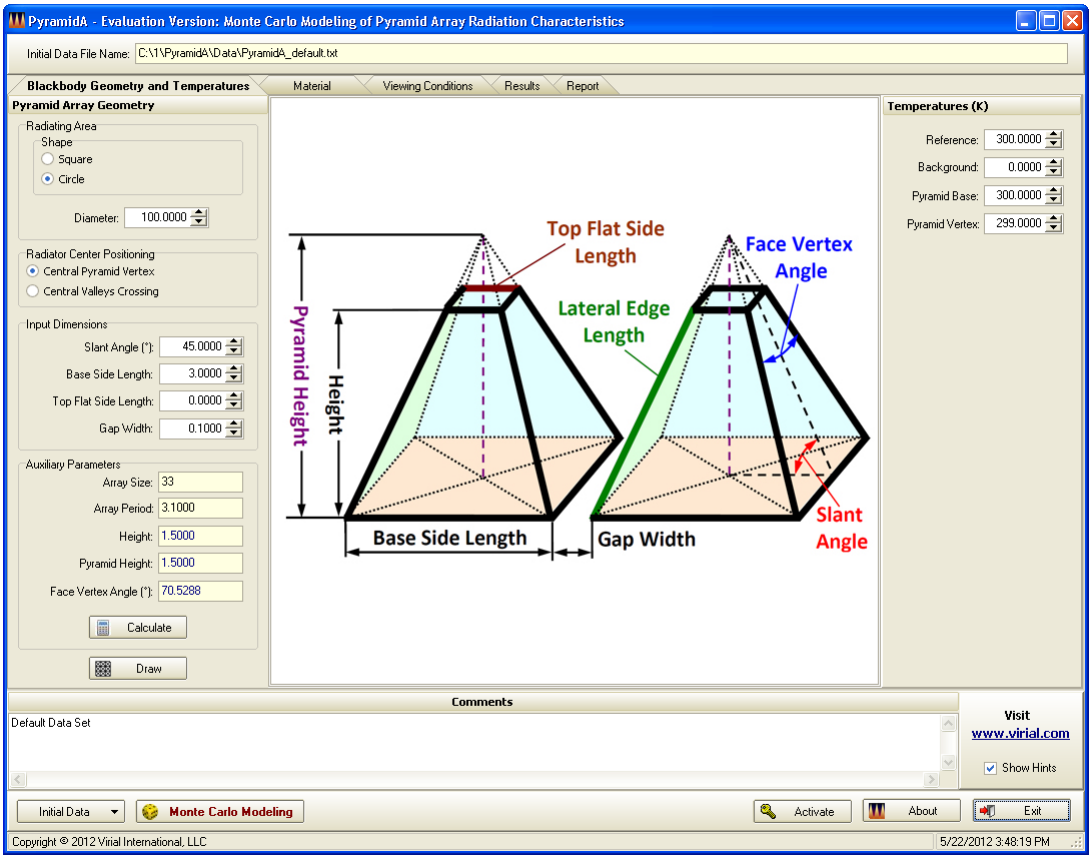

Fig. 13. **PyramidA** main window before activation (the Evaluation Version).

Simultaneously with the program start, the default data set will be loaded from the text file *PyramidA_default.txt* in the folder *Data*.

If you already purchased the license and received the activation key, you can click 

. The Activation window will appear:

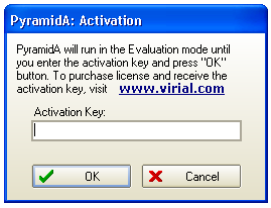

Fig. 14. Activation window

Enter the activation key then press OK. This turns Evaluation version into full-functioned program:

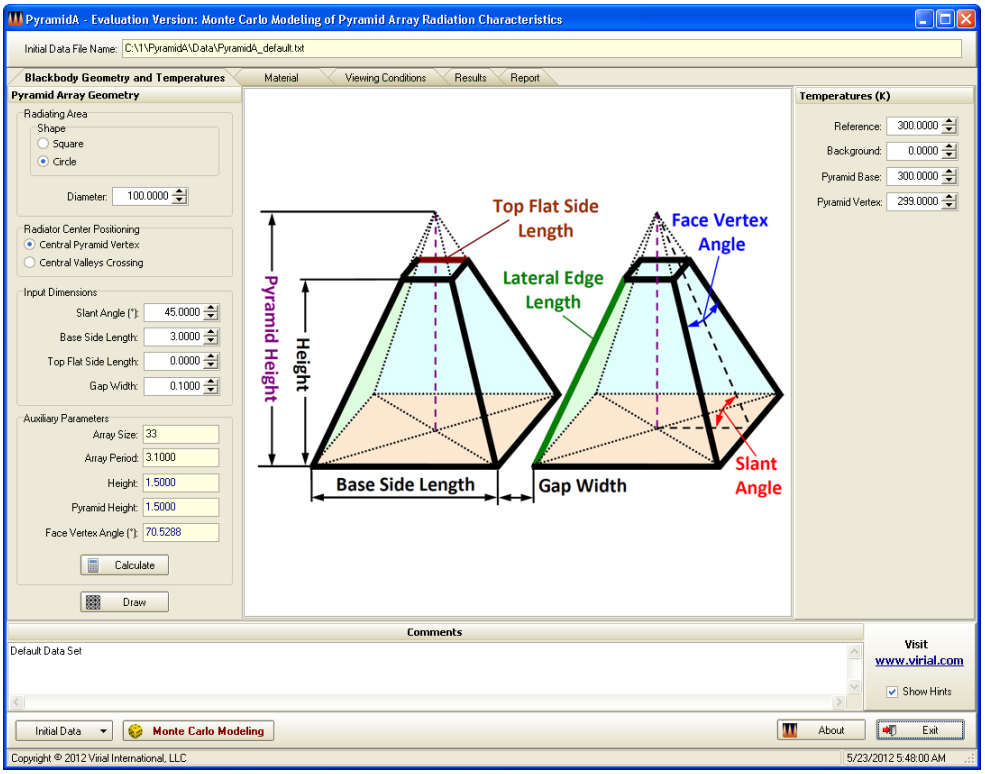

Fig. 15. **PyramidA** main window after activation (full-functioned program).

The most of the Graphical User Interface elements show pop-up hints (see an example below).

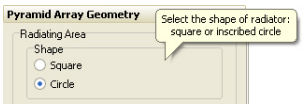

You can prevent their appearance by unchecking Show Hints in the right lower corner of the main window.

5.2. Working with Graphs

PyramidA employs two-dimensional graphs for the following purposes:

- to draw scaled top view of the PABB;
- to draw scaled top and side views of an individual pyramid;
- to visualize the targeting, i.e. preliminary ray tracing in order to verify the correctness of the viewing conditions defined;
- to plot dependences of the spectral reflectance and the spectral emissivity of the PABB surface on the wavelength;
- to plot dependences of the spectral effective emissivity and radiance temperature of PABB on wavelength.

All elements (lines, axes, legends, titles, etc.) of the PyramidA's graphs are editable.
To call the Graph Editor click Edit Graph (marked by red arrow in Fig. 16) below the graph that should be edited

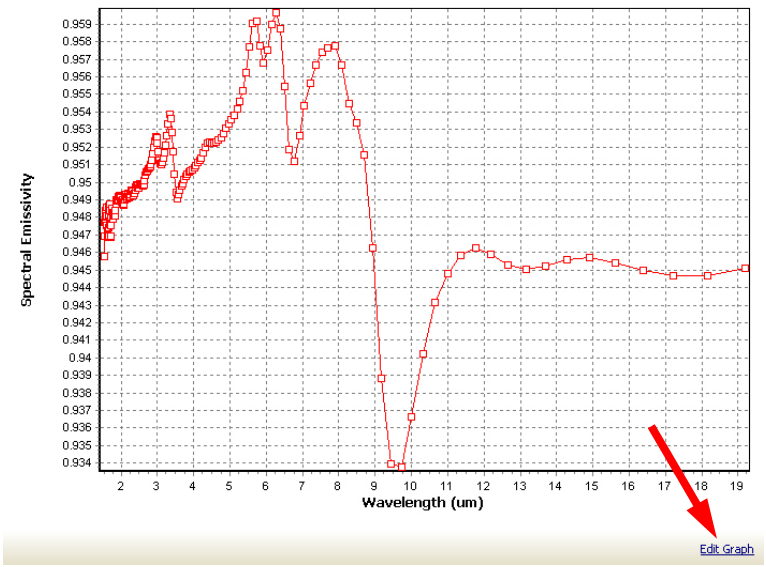

Fig. 16. An example of the editable graph.

The Graph Editor has intuitive interface (see Fig. 17) and provides comprehensive access to the editable properties of each graph allowing editing all its elements (points, axes, legend, title, etc.) and adjusting their properties. The Graph Editor gives the possibility of copying to clipboard, saving in the file, and printing graphs, as well as exporting series values in formats of text (ASCII) file, MS Excel spreadsheet, HTML and XML tables.

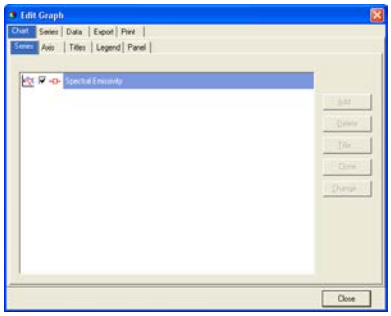

Access to individual series (lines)

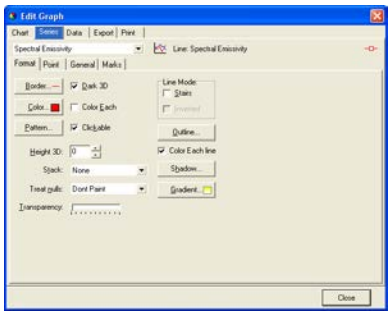

Formatting the series

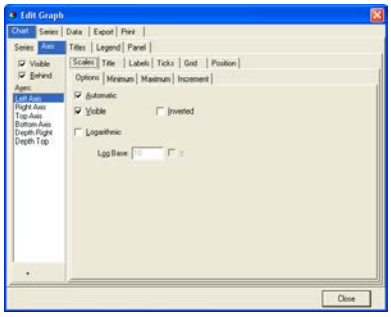

Editing the graph axes

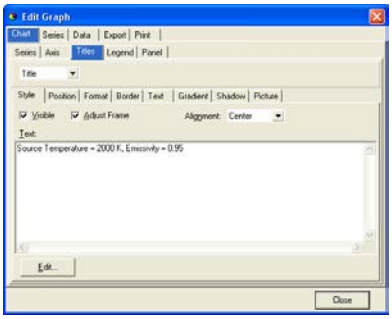

Editing the title

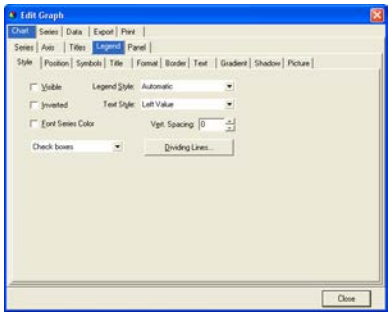

Formatting the graph legend

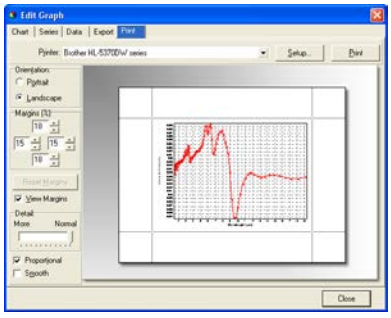

Graph printing

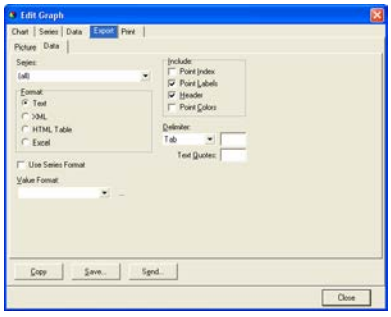

Data export

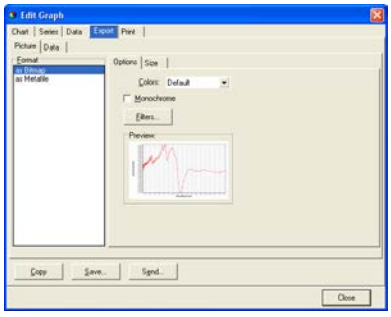

Image export

Fig. 17. Screenshots demonstrating the basic features of the Graph Editor.

PyramidA allows plotting a magnified fragment of the graph: holding left mouse button depressed, drag the cursor right and downwards to zoom (see Fig. 18) and left and upwards to unzoom.

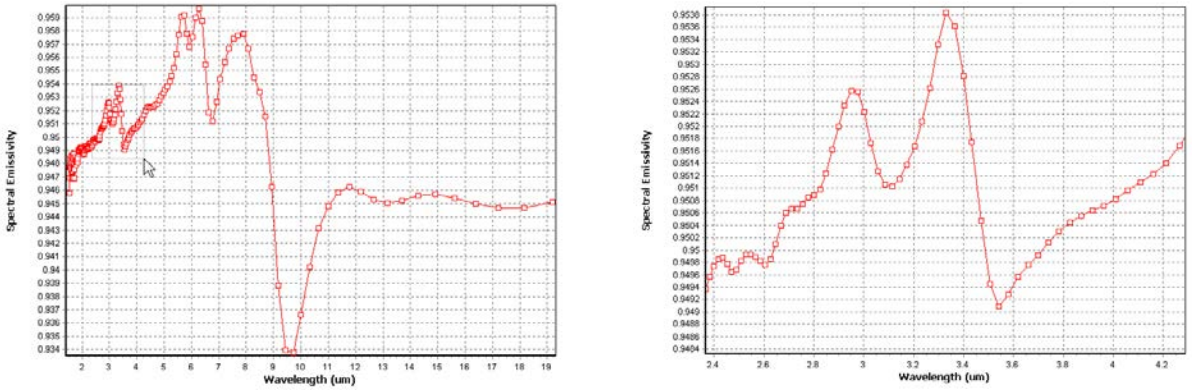

Before zoom

After zoom

Fig. 18. Use of zoom.

To displace curves relative to graph axes, hold the left mouse button depressed and move cursor. To restore graph original position, draw a rectangle of arbitrary size by moving from the bottom right corner to the top left one while left mouse button remains pressed.

5.3. Working with Tables

PyramidA's tables serve to temporary storing of spectral data (spectral reflectance and spectral emissivity of the PABB material (Fig. 19) and computed spectral effective emissivity and radiance temperatures of the PABB (Fig. 20). These tables use in-memory databases. If permanent data storing is necessary they can be saved in the text (ASCII) file. All records in PyramidA's tables are sorted in ascending order of wavelengths. To manipulate data in the tables one can use keyboard commands or the special control – the Database Navigator (Fig. 21). To move between cells of the table, use <Tab> and arrow keys, mouse or other pointer device. Non-editable (read-only) columns have yellow-colored background. Values in the column "Emissivity" of the table shown in Fig. 19 are computed automatically as soon as the values in the column "Reflectance" are entered.

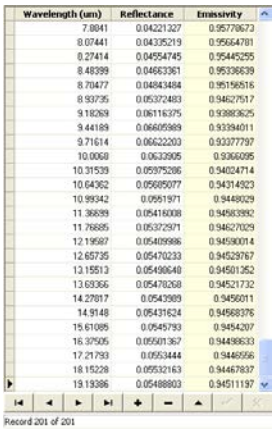

Wavelength (um)	Reflectance	Emissivity
7.8041	0.04221227	0.95778673
8.07441	0.04335219	0.95664781
8.27414	0.04554745	0.95445255
8.48399	0.04663361	0.95336639
8.70477	0.04843484	0.95156516
8.93735	0.05372483	0.94627517
9.18269	0.06116375	0.93883625
9.44189	0.06605989	0.93394011
9.71614	0.06622203	0.93377797
10.0068	0.0633905	0.9366095
10.31539	0.05975286	0.94024714
10.64362	0.05685077	0.94314923
10.99342	0.0551971	0.9448029
11.36699	0.05416008	0.94583992
11.76685	0.05372971	0.94627029
12.19587	0.05409986	0.94590014
12.65735	0.05470233	0.94529767
13.15513	0.05498648	0.94501352
13.69366	0.05478268	0.94521732
14.27817	0.0543989	0.9456011
14.9148	0.05431624	0.94568376
15.61085	0.0545793	0.9454207
16.37505	0.05501367	0.94498633
17.21793	0.0553444	0.9446556
18.15228	0.05532163	0.94467837
19.19386	0.05488803	0.94511197

Record 201 of 201

Fig. 19. Table storing the spectral reflectance and spectral emissivity of the PABB material.

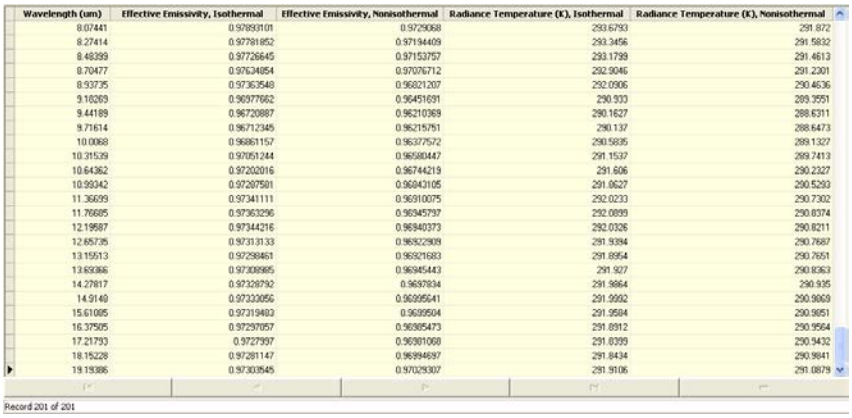

Wavelength (um)	Effective Emissivity, Isothermal	Effective Emissivity, Nonisothermal	Radiance Temperature (K), Isothermal	Radiance Temperature (K), Nonisothermal
8.07441	0.97893101	0.9729068	293.6793	291.872
8.27414	0.97781852	0.97194409	293.3456	291.5832
8.48399	0.97726645	0.97153757	293.1799	291.4613
8.70477	0.97634854	0.97076712	292.9046	291.2301
8.93735	0.97363548	0.96821207	292.0906	290.4636
9.18269	0.96977662	0.96451691	290.933	289.3551
9.44189	0.96720887	0.96210369	290.1627	288.6311
9.71614	0.96712345	0.96215751	290.137	288.6473
10.0068	0.96861157	0.96377572	290.5835	289.1327
10.31539	0.97051244	0.96580447	291.1537	289.7413
10.64362	0.97202016	0.96744219	291.606	290.2327
10.99342	0.97287501	0.96943105	291.8627	290.8293
11.36699	0.97341111	0.96910075	292.0233	290.7302
11.76685	0.97363296	0.96945797	292.0899	290.8374
12.19587	0.97344216	0.96840373	292.0326	290.8211
12.65735	0.97313133	0.96822909	291.9394	290.7687
13.15513	0.97298461	0.96921683	291.8954	290.7651
13.69366	0.97308965	0.96945443	291.927	290.8363
14.27817	0.9732872	0.9697834	291.9864	290.935
14.9149	0.97323056	0.96995641	291.9992	290.9869
15.61085	0.97319493	0.9699504	291.9584	290.9851
16.37505	0.97297057	0.96965473	291.8912	290.9564
17.21793	0.9727997	0.96901068	291.8399	290.9432
18.15228	0.97281147	0.96994697	291.8434	290.9841
19.19386	0.97303545	0.97029307	291.9106	291.0879

Record 201 of 201

Fig. 20. Table storing the computed spectral effective emissivity and radiance temperatures of the PABB. All columns are non-editable (read-only).

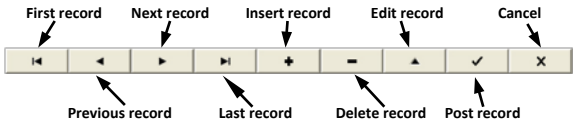

Fig. 21. The Database Navigator.

To add a new record to a table, use one of the following methods:

- Click *Insert Record* in the Database Navigator;
- Press *Insert* on the keyboard;
- Press *Down* key if you'd like to append a new record to the end of a table.

To delete a current record:

- Click “Delete Record” in the Database Navigator or
- Press “Delete” on the keyboard.

To edit a record, click *Edit Record* in the Database Navigator or directly enter the value in an input field. Usually, changes made in an edited or newly added record are saved in the database as soon as you exit from the table. However, to make sure that changed values are saved, you may click *Post Edit* in the Database Navigator. Until changes are saved, one can restore original values in an edited record by pressing *Esc* on the keyboard or by clicking *Cancel* in the Database Navigator.

All fields must have values. If you leave the field blank, the PyramidA will react by a message **Field “…” must have a value.** In this case, press “OK” button below the message then press <Esc> or click *Cancel* or *Delete* of the appropriate Database Navigator.

All data contained in the table can be loaded from and saved in the text (ASCII) file by clicking “Load” and “Save As...” items of the drop-down menus associated with the buttons 

and 

marked by the ▼ sign.

5.4. Defining Initial Data

5.4.1. Default Data Set

When PyramidA starts it automatically searches for the *PyramidA_default.txt* file in the folder *PyramidA\Data*. If this file is found it will be opened and the initial data from *PyramidA_default.txt* file will be read. So, if you're going to work with some data set for a long time (for example, during parametrical study of the PABB), it makes sense to save it under the name *PyramidA_default.txt* (see details in Section 5.4.6). Every time when you'll run PyramidA, the initial data will be automatically loaded from this file.

5.4.2. Entering PABB geometry

If you enter initial data manually (instead of loading from a text file) we recommend (this is not a mandatory requirement) to follow the order of tabbed pages arrangement as it is shown in Fig. 15. First, you have to enter geometrical parameters of the PABB:

1. Choose the shape of PABB by clicking a radio button in the group "Shape":

2. Enter the PABB diameter (if radiator has a circular shape) or square side (if radiator is square).
3. Specify whether PABB center coincides with the vertex of the central pyramid or with the inter-pyramid junction using radio buttons in the group "Radiator Center Positioning":

4. Enter all necessary dimensions included in the group "Input Dimensions":

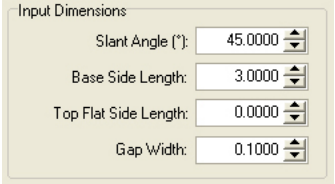

To compute and display auxiliary parameter derived from the input dimensions click Calculate. If you'd like to draw scaling views of the PABB and individual pyramid click Draw. In the latter case, the auxiliary parameters will be also calculated and the window with the scaled drawings will be opened (see Fig. 22).

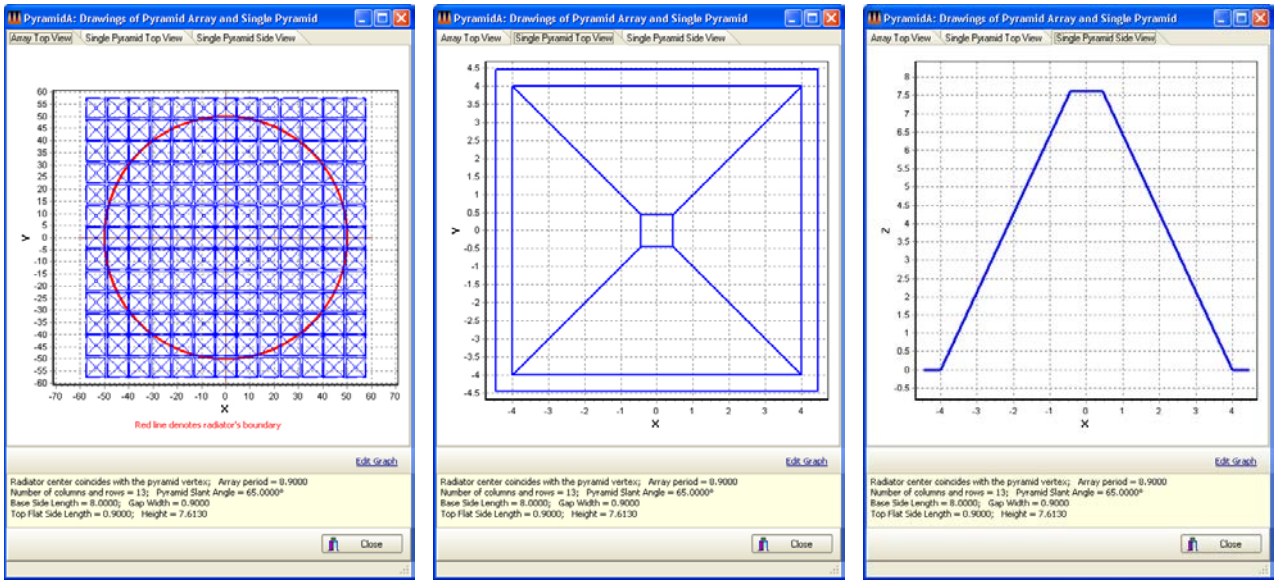

Fig. 22. The "Drawings" window.

5.4.3. Entering Temperatures

You have to enter four temperature values in Kelvins: reference, background, temperature of pyramid base (it is supposed that all PABB base is isothermal at this temperature), and temperature of pyramid vertex or top flat (if pyramids are truncated):

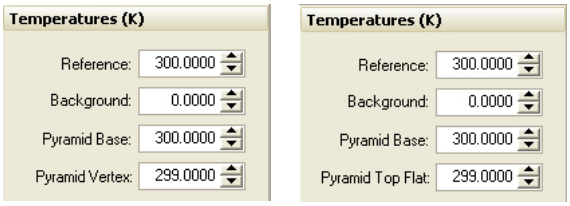

5.4.4. Entering Optical Characteristics of PABB material

It is supposed that all radiating surface of the PABB is made of the same material whose optical properties can be described in terms of uniform specular-diffuse (USD, see Section 3.3 for detail) model of reflection.

Fig. 23 shows screenshots of the tabbed page “Material”.

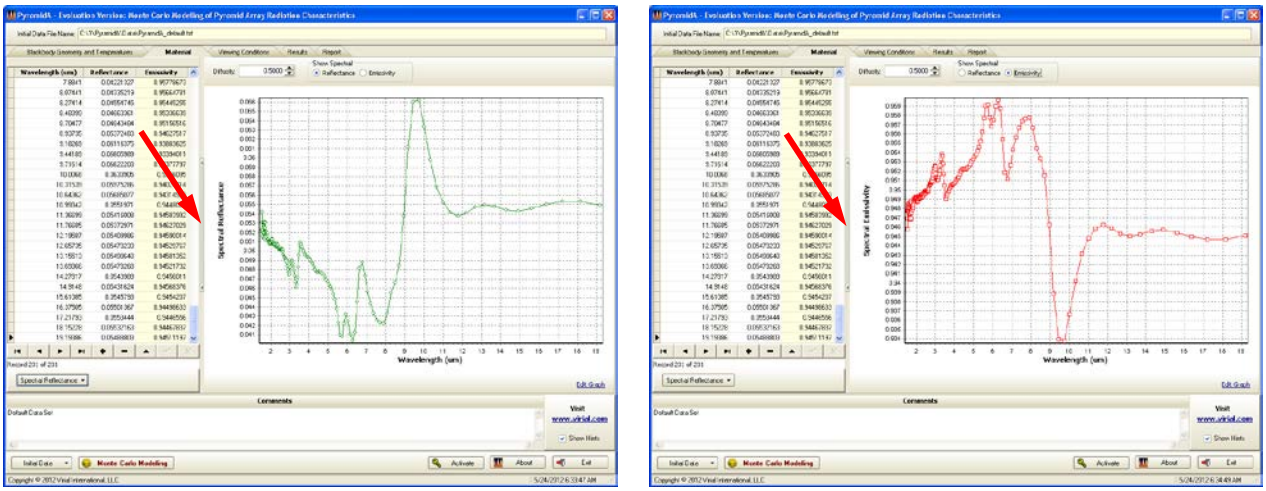

Fig. 23. The tabbed page “Material”: the plot for spectral reflectance is show on the left and for spectral emissivity – on the right. Red arrow indicates the sizing bar.

Its left part includes the table consisting of the columns “Wavelength”, “Reflectance”, and “Emissivity”, the Database Navigator, and the button Spectral Reflectance with the associated drop-down menu:

Fig. 24. The drop-down menu associated with the “Spectral Reflectance” button.

The left part of the tabbed page “Material” consists of the input field for the diffusity value, the switch

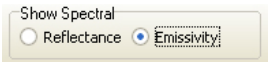

,

and the graph for displaying spectral reflectance and spectral emissivity.

Drag the sizing bar (indicated by red arrows in Fig. 23) between the left and right parts to decrease the graph width. Click the sizing bar to hide/show the left part; when it is collapsed the graph is expanded to the entire width of the tabbed page.
The "Emissivity" column of the table in the left part of the "Material" tabbed page is read-only. The value of the spectral emissivity is calculated as soon as the corresponding value of the spectral reflectance is entered in the column "Reflectance" and posted. Values in columns "Wavelength" and "Reflectance" can be entered manually or from the text file by clicking "Load" item of the drop-down menu depicted in Fig. 24. Correspondingly, "Save As…" item allows saving spectral reflectances in the text file. A fragment of such a file is presented below:

0.5 0.0635
0.65 0.0671
0.9 0.0711
1.15 0.0724
1.39 0.0729
1.55 0.0706
……
5 0.0267
5.25 0.0284
5.5 0.0318
5.75 0.0388
6 0.0426

Several other examples can be found in the folder *PyramidA**data**SR*. It is possible to prepare such a file using any text editor (e.g. MS Windows Notebook) or using MS Excel spreadsheets. In the latter case, two-column data should be saved as Text (Tab delimited).

One can define a gray (spectrally non-selective) material by clicking the "Gray" item of the drop-down menu depicted in Fig. 24. The window shown in Fig. 25 will be opened. Enter a value for the constant spectral reflectance and boundaries of the wavelength range (Min. and Max. values in μm). Then you must choose which way to defining the wavelength points uniformly distributed from Min. to Max. wavelength is more convenient for you: to specify the number of wavelength or to specify the step (increment) in μm. Both cases are shown in Fig. 25.

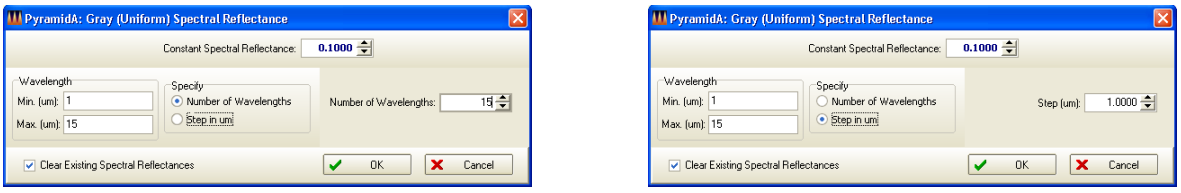

Fig. 25. Window for defining gray material for the regular wavelength grid.

After entering the number of wavelengths or step, respectively, click OK to enter wavelength-independent spectral reflectance into the table.

If you'd like to delete more than one record in the table at once it makes sense to click "Erase Multiple Records" item in the above-mentioned drop-down menu. The window shown in Fig. 26 will appear. Select the suitable radio button in the group "Records", enter (if necessary) the numbers of the first and the last records which should be erased then click OK.

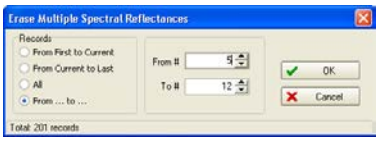

Fig. 26. Erasing more than one record at once.

5.4.5. Entering Viewing Conditions

The tabbed page "Viewing Conditions" is intended to describe geometrical conditions of collecting radiation emitted by PABB and performing targeting (see the next Section), i.e., preliminary ray tracing which allows you to verify visually the feasibility of viewing conditions you defined.

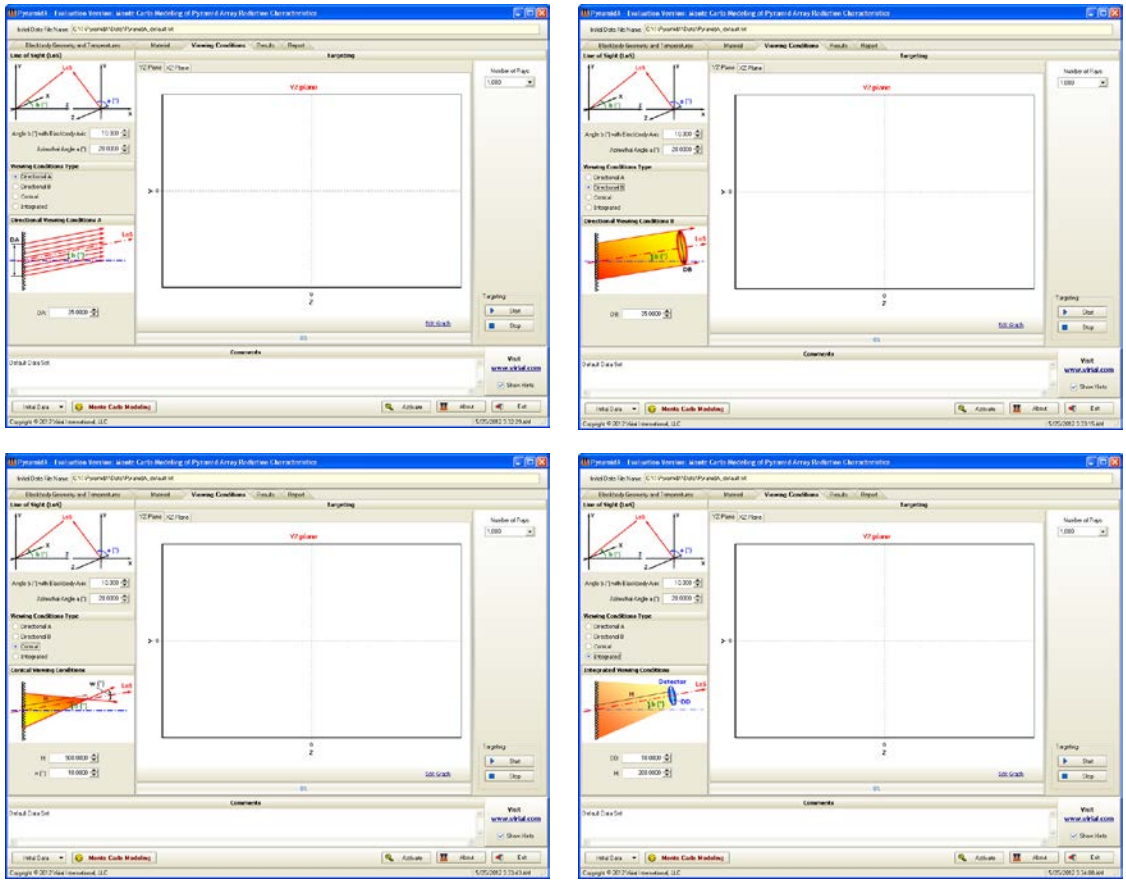

Fig. 27. The tabbed page "Viewing Conditions" for four possible types of viewing conditions.

First, you have to choose the type of the viewing conditions which are best described your task. Second, enter the polar *b* and azimuthal *a* angles (in degrees) defining the LoS direction. Then enter values of geometrical parameters for the viewing conditions type you chosen.

5.4.6. Targeting

As it was already stated, the targeting means preliminary ray tracing with relatively small number of rays. This allows visually verifying the feasibility of viewing conditions defined. Fig. 28 presents results of targeting for conical viewing conditions. Left-hand plots are for YZ plane, right-hand plots are for XZ plane. The lower plots demonstrate the use of zoom and allow defining the area of PABB (footprint) encircled by the viewing beam.

Usually, 1,000 rays are enough for the reliable targeting; however you can choose another value using the drop-down list shown below:

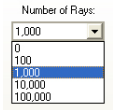

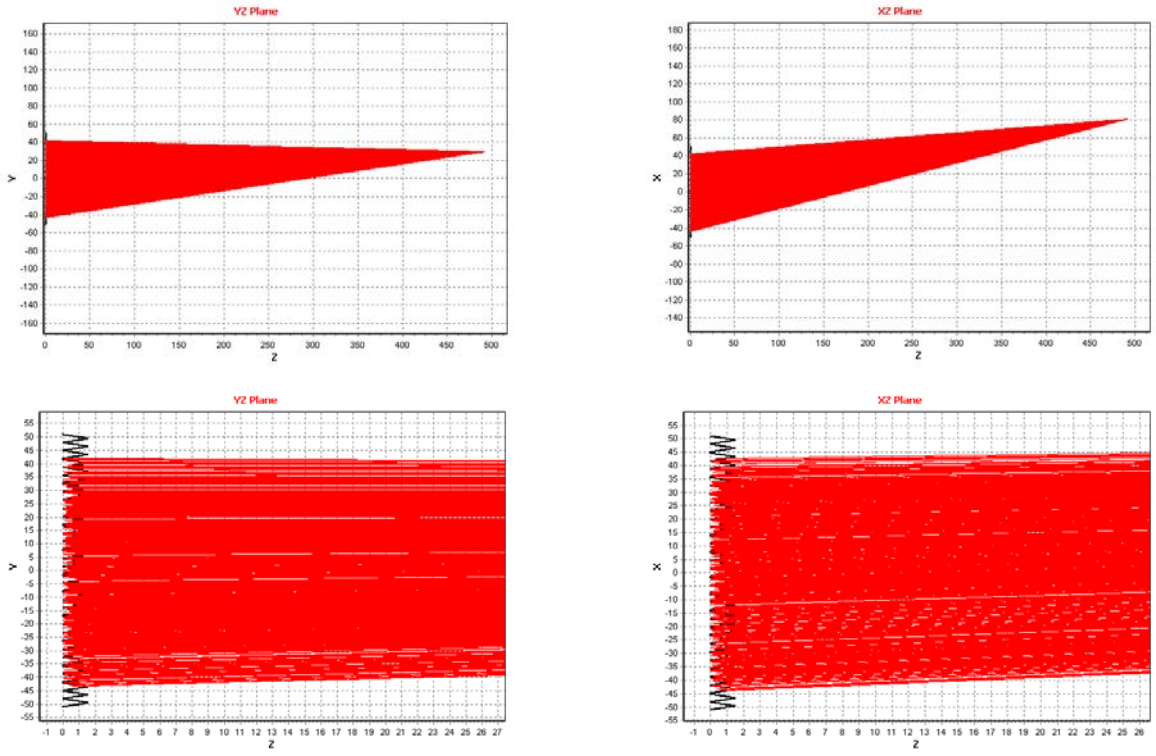

Fig. 28. Targeting results in YZ and XZ planes for conical viewing conditions (the lower plots are zoomed).

If the footprint is greater than PABB, i.e., the field-of-view (FOV) spans areas outside the PABB boundaries, the targeting is stopped and the warning message appears in the plots headers (see Fig. 29).

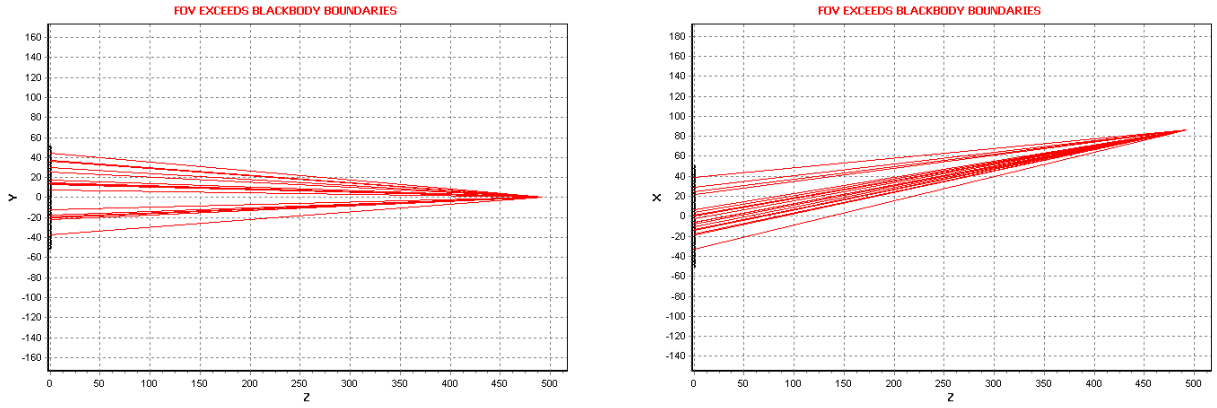

Fig. 29. The warning message appears if the footprint exceeds the PABB.

5.4.7. Comments

In order to simplify the identification of your task, you can enter arbitrary text information in the text field “Comments” in the main window lower part. This text will be saved in the text file with initial data (see the next Section) and will be included into the report (see Section 5.7).

5.4.8. Operations with Entire Data Set

Operations with the entire data set include loading, saving, and erasing and are performed using the drop-down menu

associated with the button 

.

The fastest way for data input in PyramidA is to load all data from a text file of special structure. Below, the fragment of such a file is presented.

```
2012/05/11 21:00:45  // Date and time of dataset saving
1  // Circular blackbody
  100.0000  // Blackbody diameter
0  // Radiator center coincides with the central pyramid vertex
  45.0000  // Pyramid slant angle in deg.
```

```
   3.0000  // Pyramid side length
    0.0000  // Top flat side length
   0.1000  // Gap width
  300.0000  //  Reference temperature (K)
   0.0000  //  Background temperature (K)
  300.0000  //  Radiator base temperature (K)
  299.0000  //  Pyramid top temperature in (K)
3  //  Viewing conditions index: 0 - Directional A, 1 - Directional B, 2 - Conical, 3 - Integrated
  10.0000  // Line of Sight (LoS) angle with blackbody base normal (°)
   0.0000  // Line of Sight (LoS) azimuthal angle (°)
    10.0000  // Detector diameter
   200.0000  // Distance H to the detector
 0.5000  // Diffusity of material
201  // Number of points for spectral reflectance
Wavelength (um)   Reflectance
    1.53846       0.05424585
    1.54557       0.05309866
    1.55274       0.05230570
    1.55999       0.05217749
    1.56729       0.05220026
.....................................
   15.61085       0.05457930
   16.37505       0.05501367
   17.21793       0.05534440
   18.15228       0.05532163
   19.19386       0.05488803
COMMENTS:
Default Data Set
```

Files having such a structure can be created using PyramidA or composed manually. Text starting from "//" in each line is optional and will be ignored when the file is read.

Correspondingly, to save data set you defined click "Save As..." menu item. All initial data will be saved in the text file of the structure presented above.

The "Clear All" menu item erase all data entered in the all input fields and tables of the main window. All results and graphs displayed will be also erased. It might be convenient before entering the initial data for a new task.

5.5. Monte Carlo Modeling

As soon as all initial data are defined, you can begin the Monte Carlo modeling by clicking Monte Carlo Modeling. The window shown in Fig. 30 will appear.

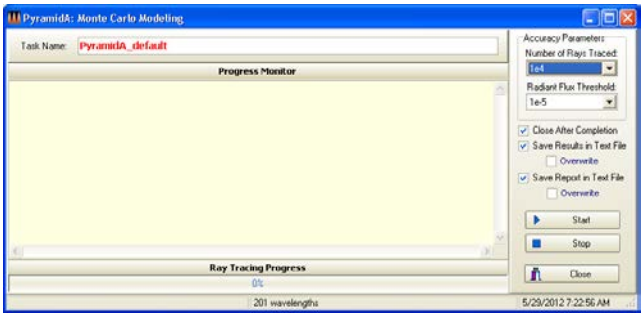

Fig. 30. The Monte Carlo Modeling window.

Now, you have to define the accuracy parameters: the number of rays traced and the radiant flux threshold (see Fig. 31).

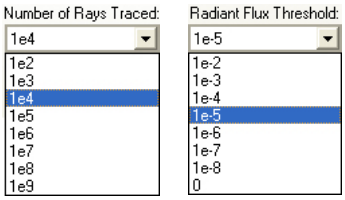

Fig. 31. Drop-down lists for defining the accuracy parameters.

The number n of rays traced determines the stochastic uncertainty of the Monte Carlo modeling. The greater number of rays traced the lower the random error in calculation results: according to the common rule, the random error of the effective emissivity is in inverse proportion of $\sqrt{n}$. Usually, 10^5…10^6 rays provide accuracy sufficient for the most applications.

The radiant flux threshold γ prescribes when the tracing of a ray can be terminated. There are no reasons to continue tracing of the ray if it carries too small fraction of its initial energy. So, if the required precision of the effective emissivity calculation is of 10^{-4}, there is no necessity to continue tracing the ray which transfers only 10^{-6} of its initial radiant flux. We recommend to set γ 10 times less than the precision required. Setting $\gamma = 0$ completely eliminates this problem but can lead to the unreasonable increased calculation time.

Checkboxes below the accuracy parameters input fields allow to manage the behavior of PyramidA after completion of calculations. When checkboxes “Close After Completion”, “Save Results in Text File”, and “Save Report in Text File” are checked, the Monte Carlo Modeling window will be closed after calculations, the results obtained and the report composed will be saved in text files under the name specified in the “Task Name” field. If checkboxes “Overwrite” are unchecked, PyramidA asks confirmations for files rewriting (if they exist). Otherwise, the results and report files will be rewritten without confirmation requests.
Now, you can click Start to start ray tracing. It can be interrupted at any time by clicking Stop. Before starting the ray tracing, PyramidA preprocesses initial data; operations performed are displayed in the Progress Monitor (see Fig. 32).

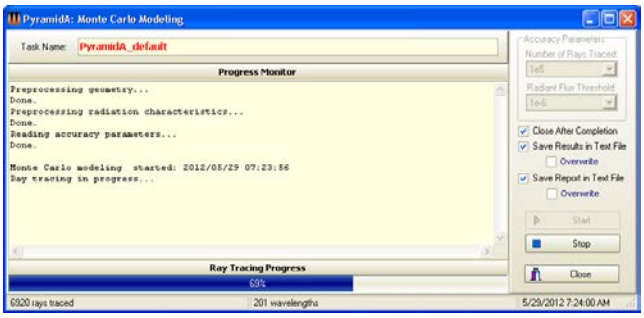

Fig. 32. Ray tracing in progress.

5.6. Viewing and Saving Results

If the checkbox ☑ Close After Completion is checked, the "Monte Carlo Modeling" window will be closed after finishing the ray tracing. The Main window will display the graph for the spectral emissivities One can switch between displaying dependences on wavelength for spectral effective emissivity and radiance temperature using the Effective Emissivity/Radiance Temperature radio buttons group (see Fig. 33).

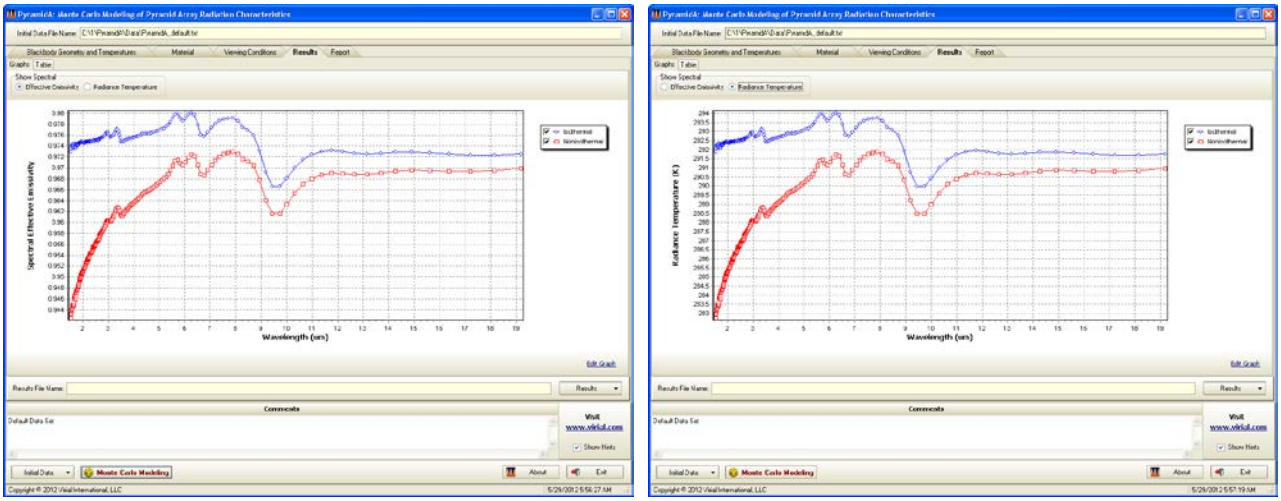

Fig. 33. Computed dependence of the spectral effective emissivity (left) and the radiance temperature (right) on wavelength.

The tabbed sub-page "Table" contains the table with the results of the Monte Carlo modeling (see Fig. 34).

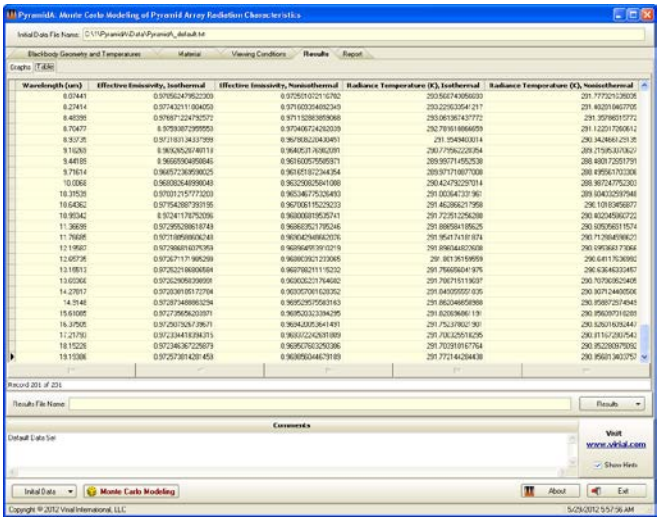

Fig. 34. Tabular representation of calculation results.

The drop-down menu

associated with the button 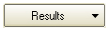

allows to perform standard actions with the calculation results. They can be saved in and load from the text file. Below, you can find a fragment of such a file; other examples can be found in the folder *PyramidA\Results*.

Wavelength (um)	EEIso	EENoniso	RTIso (K)	RTNoniso (K)
1.00000	0.99621771	0.98188972	398.4871	392.7559
1.10000	0.99642483	0.98336734	398.5699	393.3469
1.20000	0.99662792	0.98463112	398.6512	393.8524
1.30000	0.99682712	0.98572924	398.7308	394.2917
1.40000	0.99689267	0.98657651	398.7571	394.6306
1.54000	0.99693832	0.98755077	398.7753	395.0203
.....				
14.92000	0.99693181	0.99716323	398.7727	398.8653
15.62000	0.99691878	0.99723366	398.7675	398.8935
16.38000	0.99688614	0.99729326	398.7545	398.9173
17.22000	0.99686650	0.99736105	398.7466	398.9444
18.16000	0.99686650	0.99744039	398.7466	398.9762
19.20000	0.99689921	0.99753556	398.7597	399.0142
20.00000	0.99688614	0.99758393	398.7545	399.0336

PyramidA allows reading, displaying, and plotting previously saved results files.

Erasing of multiple records is performed in the same way as it was described for spectral reflectances in Section 5.4.4.

5.7. Viewing and Saving the Report

PyramidA's report contains all initial data as well as calculation results in the text (ASCII) format. Report is created automatically after completion the Monte Carlo modeling. Fig. 35 shows the tabbed page "Report". Normally, report is non-editable (read-only). If you'd like to edit it (for instance, to append additional comments) you must previously uncheck Read Only.

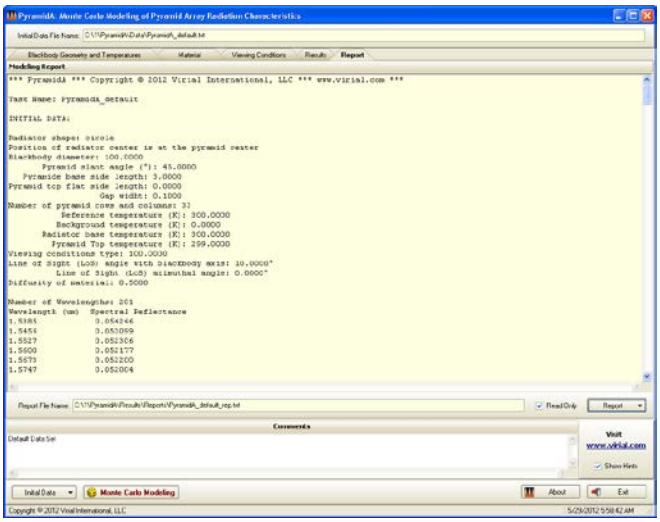

Fig. 35. The tabbed page "Report".

The drop-down menu

associated with the button Report allows to perform the same standard actions as in the case of calculation results. Below, a fragment of the text file containing the report is shown. Other examples of report files can be found in the folder *PyramidA\Results\Reports*.

***** PyramidA *** Copyright © 2012 Virial International, LLC *** www.virial.com *****

Task Name: Example 1

INITIAL DATA:

Radiator shape: square
Position of radiator center is at the pyramid center
Blackbody side: 100.0000
Pyramid slant angle (°): 60.0000
Pyramide base side length: 5.0000
Pyramid top flat side length: 0.0000
Gap widht: 0.0000
Number of pyramid rows and columns: 21
Reference temperature (K): 400.0000
Background temperature (K): 300.0000
Radiator base temperature (K): 400.0000
Pyramid Top temperature (K): 399.5000

Viewing conditions type: Conical
Line of Sight (LoS) angle with blackbody axis: 0.0000°
Line of Sight (LoS) azimuthal angle: 0.0000°
Distance H to the focal point: 150.0000
FOV (viewing cone vertex angle): 10.000°
Diffusity of material: 0.1000

Number of Wavelengths: 92
Wavelength (um) Spectral Reflectance
1.0000 0.065000
1.1000 0.062000
1.2000 0.059000
1.3000 0.056000
……
14.2800 0.054400
14.9200 0.054400
15.6200 0.054600
16.3800 0.055100
17.2200 0.055400
18.1600 0.055400
19.2000 0.054900
20.0000 0.055100

COMMENTS:

Example #1.
Square radiator centered
at the pyramid vertex.
60-deg. pyramid array 21 x 21
without gaps and flats.
Almost specular selective
high-emissivity paint within
1.5 - 20 um.
Tref = 400 K
Tbg = 300 K
Tbase = 400 K
TTop = 399.5 K
Normal viewing conditions.

Number of rays: 10000000
Radiant flux threshold: 0.00000100

Monte Carlo modeling started: 2012/05/12 06:25:17
Monte Carlo modeling finished: 2012/05/12 07:34:03

RESULTS:

WL (um)	EEIso	EENoniso	RTIso (K)	RTNoniso (K)
1.0000	0.99621771	0.98188972	398.4871	392.7559
1.1000	0.99642483	0.98336734	398.5699	393.3469
1.2000	0.99662792	0.98463112	398.6512	393.8524
1.3000	0.99682712	0.98572924	398.7308	394.2917
1.4000	0.99689267	0.98657651	398.7571	394.6306
……				
13.7000	0.99690574	0.99699463	398.7623	398.7979
14.2800	0.99693181	0.99708595	398.7727	398.8344
14.9200	0.99693181	0.99716323	398.7727	398.8653
15.6200	0.99691878	0.99723366	398.7675	398.8935
16.3800	0.99688614	0.99729326	398.7545	398.9173
17.2200	0.99686650	0.99736105	398.7466	398.9444
18.1600	0.99686650	0.99744039	398.7466	398.9762
19.2000	0.99689921	0.99753556	398.7597	399.0142
20.0000	0.99688614	0.99758393	398.7545	399.0336

PyramidA allows also reading and displaying previously saved report files.

6. EVALUATION VERSION VS. FULL-FUNCTIONED PROGRAM

PyramidA will work in the Evaluation mode until you activate it by entering the activation key you'll obtain as soon as the license will be purchased. Evaluation Version of **PyramidA** uses the same computational procedures as the full-functioned program but has several restrictions:

1. Evaluation version allows tracing only 100 rays;
2. Flux threshold is always equal to 0.01;
3. No randomization is performed before ray tracing.

These restrictions make impossible obtaining precise results using the Evaluation version. After clicking Monte Carlo Modeling, the Evaluation version of PyramidA shows the Warning window shown in Fig. 36.

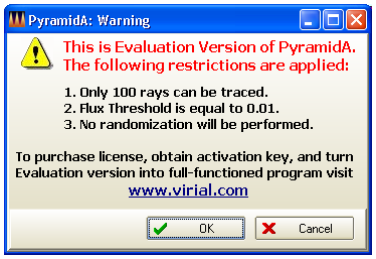

Fig. 36. The Warning window of the Evaluation version.

Procedure of activation **PyramidA** is described in Section 5.1.

7. REFERENCES

1. S. H. S. Wilson, N. C. Atkinson, and J. A. Smith, "The Development of an Airborne Infrared Interferometer for Meteorological Sounding Studies," Journal of Atmospheric and Oceanic Technology **16**, 1912-1927 (1999).

2. A. Kuze, H. Suto, M. Nakajima, and T. Hamazaki, "Thermal and near infrared sensor for carbon observation Fourier-transform spectrometer on the Greenhouse Gases Observing Satellite for greenhouse gases monitoring," Appl. Opt. **48**, 6716-6733 (2009).

3. B. Gutschwager, H. Driescher, J. Herrmann, H. Hirsch, J. Hollandt, H. Jahn, P. Kuchling, C. Monte, and M. Scheiding, " Characterization of the 300 K and 700 K Calibration Sources for Space Application with the Bepicolombo Mission to Mercury," Int. J. Thermophys. **32**, 1429-1439 (2011).

4. D. Blumstein, G. Chalon, T. Carlier, C. Buil, Ph. Hébert, T. Maciaszek, G. Ponce, T. Phulpin, B. Tournier, D. Siméoni, P. Astruc, A. Clauss, G. Kayal, and R. Jegoue, "IASI instrument: Technical overview and measured performances," Proc. SPIE **5543**, 22 (2004).

5. Temperature Calibration Equipment & Services. Isothermal Technology Limited. Pine Grove, Southport, Merseyside PR9 9AG England (www.isotech.co.uk).

6. http://www.hgh.fr/corps-noir-etendu-infrarouge-infrared-source-extended-blackbody-en.php

7. B. H. Lambrigtsen, "Calibration of the AIRS Microwave Instruments," IEEE Trans. Geosci. Rem. Sens. **41**, 369-378 (2003).

8. J. Randa, D. K. Walker, A. E. Cox, and R. L. Billinger, "Errors Resulting From the Reflectivity of Calibration Targets," IEEE Trans. Geosci. Rem. Sens. **43**, 50-58, (2005).

9. J. Randa, A. E. Cox, and D. K. Walker, "Proposal for Development of a National Microwave Brightness-Temperature Standard," Proc. SPIE **6301**, 05 (2006).

10. N. Feng and W. Wei, "The Optimization Design for Microwave Wide Band Blackbody Calibration Target," Proc. IEEE International Conference on Microwave and Millimeter Wave Technology (ICMMT 2008), Nanjing, 13 June 2008, vol. **4**, 1695 - 1698 (2008).

11. A. Murk, A. Duric, and F. Patt, "Characterization of ALMA Calibration Targets," Proc. 19th International Symposium on Space Terahertz Technology, Groningen, 28-30 April 2008, 530-533 (2008).

12. T. J. Quinn, “A practical black-body cavity for the calibration of radiation pyrometers,” J. Sci. Instrum. **44,** 221-222 (1967).

13. G. Machin and B. Chu, “A Transportable Gallium Melting Point Blackbody for Radiation Thermometry Calibration,” Meas. Sci. Technol. **9**, 1653–1656 (1998).

14. S. Gu, G. Fu, and Q. Zhang, “3500-K High-Frequency Induction-Heated Blackbody Source,” J. Thermophysics **3**, 83-85 (1989).

15. M. Battuello, V. Chimenti, G. Machin, H. C. McEvoy, J. Perez, T. Ricolfi, and R. Sergienko, “A Comparison of the Primary Standard Zinc Point Blackbody Cavities of NPL and CEM with IMGC,” Proc. TEMPMEKO 2001, Vol. 2, 857-862 (VDE Verlag GMBH, Berlin – Offenbach, 2001).

16. B. Chu , H. McEvoy, and G. Machin, “Use of an InGaAs Radiation Thermometer To Verify the Accuracy of the NPL Blackbody Reference Sources from 156°C to 600 °C,” in: Temperature: Its Measurement and Control in Science and Industry, Vol. 7, edited by D. C. Ripple, 571-576 (2003).

17. H. C. McEvoy, G. Machin, R. Friedrich, J. Hartmann, and J. Hollandt, “Comparison of the New NPL Primary Standard Ag Fixed Point Blackbody Source with the Primary Standard Fixed Point of PTB,” in: Temperature: Its Measurement and Control in Science and Industry, Vol. 7, edited by D. C. Ripple, 909-914 (2003).

18. A. Abdulkadir and R. C. Birkebak, “Spectral Directional Emittance of Metal Surfaces with Pyramidal Surface Undulation”, Proc. 5th Int. Heat Transfer Conf., 21–25 (Tokyo, 1974).

19. A. Abdulkadir and R. C. Birkebak, “Effects of Large Pyramidal Surface Roughness on Spectral Directional Emittance,” Warme- und Stoffubertragung **10**, 23–32 (1977).

20. A. Abdulkadir and R. C. Birkebak, “Spectral Directional Emittance of Rough Metal Surfaces: Comparison Between Semi-Random and Pyramidal Surface Approximations,” 2nd AIAA/ASME Thermophysics and Heat Transfer Conference (Palo Alto, CA, May 24-26, 1978) – 5 p.

21. P. J. Mohr, B. N. Taylor, and D. B. Newell, “The Fundamental Physical Constants,” Phys. Today **60**, 55 (2007).

22. *International Lighting Vocabulary*. 4th Edition. CIE Publication No. 17.4 (1987)/International Electrotechnical Vocabulary. Chapter 845: Lighting – International Electrotechnical Commission. Publication 50(845), Geneva, Switzerland (1987).

23. *Nomenclature and Definitions for Illuminating Engineering. American National* Standard – Transactions of the Illuminating Engineering Society of North America. ANSI/IES RP–16–1986 (ANSI Standard Z7.1–1967).

24. Y. Ohwada, “Numerical calculation of bandlimited effective emissivity,” Appl. Optics **24**, 280-283 (1985).

25. V. B. Khromchenko, S. N. Mekhontsev, and L. M. Hanssen, “Design and Evaluation of Large-Aperture Gallium Fixed-Point Blackbody,” Int. J. Thermophys. **30**, 9-19 (2009).

26. A. F. Sarofim and H. C. Hottel, “Radiation Exchange among non-Lambert Surfaces,” J. Heat Transfer, **88C**, 37–44 (1964).

27. A. Ono, “Calculation of the Directional Emissivities of the Cavities by the Monte Carlo Method,” J. Opt. Soc. Am. **70**, 547–554 (1980).

28. R. E. Bedford, “Calculation of effective emissivities of cavity sources of thermal radiation,” in Theory and Practice if Radiation Thermometry, D. P. DeWitt and G. D. Nutter, eds. (Wiley, 1988), pp. 653–772.

29. A. V. Prokhorov, L. M. Hanssen, and S. N. Mekhontsev, “Calculation of the radiation characteristics of blackbody radiation sources,” in Radiometric Temperature Measurements: I. Fundamentals, Z. M. Zhang, B. K. Tsai, and G. Machin, eds. (Academic, 2010), Vol. 42, pp. 181–240.

30. J. R. Mahan, *Radiation heat transfer: a statistical approach* (Wiley, 2002).

31. A. V. Prokhorov, “Monte Carlo method in optical radiometry,” Metrologia **35**, 465-471 (1998).

8. End-User License Agreement

License

1. Under this End-User Software License Agreement (the "EULA"), Virial International, LLC (the "Vendor") grants to the user (the "Licensee") a non-exclusive and non-transferable license (the "License") to use PyramidA (the "Software").

2. "Software" includes the executable computer programs, related electronic documentation and any other files that accompany the product.

3. Title, copyright, intellectual property rights and distribution rights of the Software remain exclusively with the Vendor. Intellectual property rights include the look and feel of the Software. This EULA constitutes a license for use only and is not in any way a transfer of ownership rights to the Software.

4. The Software may be loaded onto no more than three computers. A single copy may be made for backup purposes only.

5. The rights and obligations of this EULA are personal rights granted to the Licensee only. The Licensee may not transfer or assign any of the rights or obligations granted under this EULA to any other person or legal entity. The Licensee may not make available the Software for use by one or more third parties.

6. The Software may not be modified, reverse-engineered, or de-compiled in any manner through current or future available technologies.

7. Failure to comply with any of the terms under the License section will be considered a material breach of this EULA.

License Fee

8. The original purchase price paid by the Licensee will constitute the entire license fee and is the full consideration for this EULA.

Limitation of Liability

9. The Software is provided by the Vendor and accepted by the Licensee "as is". Liability of the Vendor will be limited to a maximum of the original purchase price of the Software. The Vendor will not be liable for any general, special, incidental or consequential damages including, but not limited to, loss of production, loss of profits, loss of revenue, loss of data, or any other business

or economic disadvantage suffered by the Licensee arising out of the use or failure to use the Software.
10. The Vendor makes no warranty expressed or implied regarding the fitness of the Software for a particular purpose or that the Software will be suitable or appropriate for the specific requirements of the Licensee.

11. The Vendor does not warrant that use of the Software will be uninterrupted or error-free. The Licensee accepts that software in general is prone to bugs and flaws within an acceptable level as determined in the industry.

Warrants and Representations

12. The Vendor warrants and represents that it is the copyright holder of the Software. The Vendor warrants and represents that granting the license to use this Software is not in violation of any other EULA, copyright or applicable statute.

Acceptance

13. All terms, conditions and obligations of this EULA will be deemed to be accepted by the Licensee ("Acceptance") on installation of the Software.

Term

14. The term of this EULA will begin on Acceptance and is perpetual.

Termination

15. This EULA will be terminated and the License forfeited where the Licensee has failed to comply with any of the terms of this EULA or is in breach of this EULA. On termination of this EULA for any reason, the Licensee will promptly destroy the Software or return the Software to the Vendor.

Force Majeure

16. The Vendor will be free of liability to the Licensee where the Vendor is prevented from executing its obligations under this EULA in whole or in part due to Force Majeure, such as earthquake, typhoon, flood, fire, and war or any other unforeseen and uncontrollable event where the Vendor has taken any and all appropriate action to mitigate such an event.

Governing Law

17. The Parties to this EULA submit to the jurisdiction of the courts of the State of Maryland for the enforcement of this EULA or any arbitration award or decision arising from this EULA. This EULA will be enforced or construed according to the laws of the State of Maryland.

Miscellaneous

18. This EULA can only be modified in writing signed by both the Vendor and the Licensee.

19. This EULA does not create or imply any relationship in agency or partnership between the Vendor and the Licensee.

20. Headings are inserted for the convenience of the parties only and are not to be considered when interpreting this EULA. Words in the singular mean and include the plural and vice versa. Words in the masculine gender include the feminine gender and vice versa. Words in the neuter gender include the masculine gender and the feminine gender and vice versa.

21. If any term, covenant, condition or provision of this EULA is held by a court of competent jurisdiction to be invalid, void or unenforceable, it is the parties' intent that such provision be reduced in scope by the court only to the extent deemed necessary by that court to render the provision reasonable and enforceable and the remainder of the provisions of this EULA will in no way be affected, impaired or invalidated as a result.

22. This EULA contains the entire EULA between the parties. All understandings have been included in this EULA. Representations which may have been made by any party to this EULA may in some way be inconsistent with this final written EULA. All such statements are declared to be of no value in this EULA. Only the written terms of this EULA will bind the parties.

23. This EULA and the terms and conditions contained in this EULA apply to and are binding upon the Vendor's successors and assigns.

Notices

24. All notices to the Vendor under this EULA are to be provided at the following address:

Virial International, LLC
538 Palmspring Dr.,
Gaithersburg, MD 20878-2972
USA

Email: info@virial.com